LUND UNIVERSITY

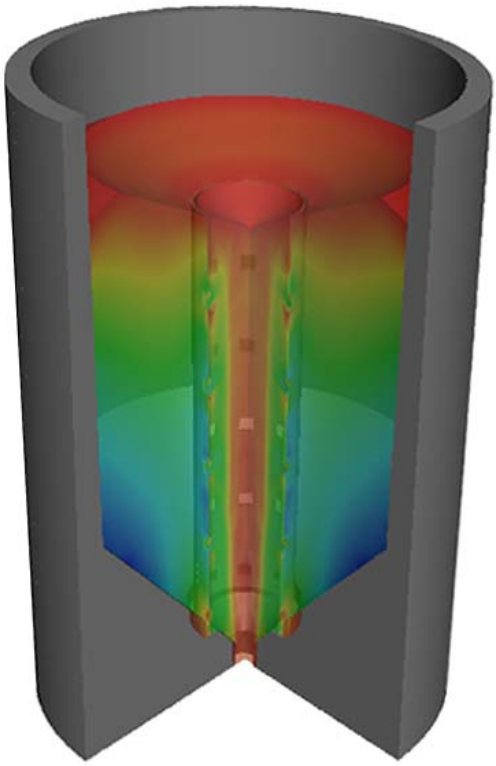

NUMERICAL ANALYSIS OF SILO DISCHARGE

JOHN BROWN

Structural Mechanics

Master's Dissertation

Department of Construction Sciences
Structural Mechanics

ISRN LUTVDG/TVSM--07/5151--SE (1-61)
ISSN 0281-6679

NUMERICAL ANALYSIS OF SILO DISCHARGE

Master's Dissertation by

JOHN BROWN

Supervisors:

Ola Dahlblom, Professor, and Per-Erik Austrell, Lecturer,
Div. of Structural Mechanics

Examiner:

Göran Sandberg, Professor,
Div. of Structural Mechanics

Printed by KFS I Lund AB, Lund, Sweden, January, 2008.

For information, address:
Division of Structural Mechanics, LTH, Lund University, Box 118, SE-221 00 Lund, Sweden.
Homepage: http://www.byggmek.lth.se

Abstract

A silo discharge with a bulk material consisting of iron ore pellets is studied. The silo is about 65 meters high and 38 meters wide. The quality of pellets decreases when they are exposed to high stresses while moving. The stresses are therefore not allowed to exceed a certain threshold. It must also be possible to trace the origin of a sample from the discharge. To fulfill these two demands the original design of the silo has a perforated inner tube to obtain a specific flow pattern.

The simulations are performed using the finite element method with the pellets as a continuum in three dimensions. The constitutive relation used for the pellets is the Drucker-Prager plasticity model. The simulations are performed with the commercial software ABAQUS/Explicit and a pure Eulerian adaptive mesh. The preliminary original design is simulated together with proposed modified designs that benefit pellet quality.

The result of the original design exceeds the threshold stress level and lacks the possibility to trace the sample's origin. Of the investigated modified designs there is one that shows lower stresses and improved traceability; a silo where the inner tube has a smaller radius than the original design.

Keywords: Granular flow, Silo, Iron ore pellets, Inner tube, FEM, ABAQUS.

Contents

Part I

Introduction

Chapter 1

Introduction

In the north of Sweden the state owned company Luossavaara-Kiirunavaara Aktiebolag, (LKAB), is increasing their production of iron ore pellets. The pellets have a shape of a sphere of about one centimeter in diameter. They have a high content of iron and are to be used in furnaces and direct reduction processes in steelworks.

Most of the pellets are shipped by boat from the harbour of Narvik in Norway. They are transported to the harbour by train on the railroad called Malmbanan. In 2008 the railroad will have a total capacity of 6800 tons per train set compared to the load of today at 4100 tons. The handling of the pellets in Narvik will be expanded to manage the heavier trains and the larger volumes.

12 large silos are going to be blasted in the bedrock with their upper level in line with the ground level. The purpose is that the trains will be able to unload their cargo directly in the top of the silo, in what is called a rolling discharge. The silo itself is then discharged in the bottom and the pellets are transported to the ships on a belt conveyor in a tunnel.

Each silo is 38 meters wide and about 65 meters high, which makes a total capacity of 110 000 tons, 50 000 cubic meters or 16 full train set of pellets. The belt conveyor is going to transport 10 000 tons per hour to the ships during a 13 hour long discharge.

The pellets have a quality measurement parameter, LTD, that should not be changed by the treatment in the silos. LKAB has consulted the Technical University of Luleå to find a relation between the handling of the pellets and an eventual change in LTD. The university found that there could be a connection between a decrease in LTD and pellets in movement combined with stress influence. LKAB has chosen a limit of vertical stress on pellets in movement to 250 kPa. Moreover they found that high static stress or high falls does not affect the quality of the pellets.

The LTD value is continuously measured during the discharge. If a change in LTD is detected, it has to be possible to track the sample back though the chain of logistics and evaluate the problem. Therefore it is desirable to have knowledge of the flow pattern in the silo. This is called the traceability criterion.

1.1 Objective

There are two objectives in this thesis; the first is to determine the stresses in the pellets and the second is to prove that the silo fulfills the traceability criterion. Both of them during discharge.

Simulating the discharge of a silo will determine the stresses and compare this to a threshold value. If the stresses exceed these values, or if the traceability criterion fails, different modifications will be analyzed to find a better solution. The modifications will mainly be geometrical changes.

The work will be performed using the commercial finite element software ABAQUS.

1.2 Delimitations

The stresses in the silo will be compared with the stated value of 250 kPa vertical stress determined by LKAB. A more detailed investigation of the stresses inside the individual pellet or what is causing the decreasing quality are not processed.

There is a possibility to discuss different types of stress in the criterion because of uncertainties in the expression vertical stress.

Concerning the traceability criterion for the silo there is no delimitation.

All simulations assume that the pellets are filled symmetrically into the silo. No asymmetric load will therefore be investigated.

1.3 Disposition

The disposition is divided into four parts. First there is a presentation of the project and its background. The second part presents the theory together with the methodology that are used in the simulations.

The results from the simulations are then presented in the third part, The Result, which is divided into two chapters, the first investigates the original design at different states and the second chapter that investigates different modified designs.

The fourth and last part is a summary of the entire work.

Chapter 2

Project presentation

In the harbour of Narvik 12 large silos are being built at a total cost of about one billion SEK. The silos are supposed to be ready in the first quarter of 2009. A computer model is shown in Figure 2.1 illustrating the railway, the silos and the underlying tunnel containing the belt conveyor for pellet transportation towards the ships. For a better apprehension of the dimensions, photos were taken on the site and shown in Figure 2.5 and 2.6.

Figure 2.1: *Principal model of the silos in the site located in the harbour of Narvik. Image courtesy LKAB.*

2.1 Iron ore pellets

Iron ore pellets are centimeter sized spheres with high iron content and uniform quality. They have a quality measurement denoted by LTD which is an abbreviation for Low Temperature Degradation. The degradation refers the process in a furnace. A closeup picture of iron ore pellets is found to the left in Figure 2.2

Figure 2.2: *Left: A closeup picture of iron ore pellets. Image courtesy LKAB. Right: The arrangement of the rubber cylinder containing iron ore pellets during shear test [6].*

From a hypothesis about mechanical influence on LTD, a series of tests were performed at Luleå University of Technology. The pellets were put into a rubber cylinder, which was loaded with an axial load, and sheared in one or both directions. The arrangement is seen to the right in Figure 2.2. The result can show some initial decrease in LTD for axial loads around 400 kPa. There are still questions about the influence of the conditions in the pellets before the tests and about the real stress condition in the cylinder during the tests. The exact cause to the decrease in LTD is therefore not fully known. The stress limit for the design of the silo is set to 250 kPa from the evaluation of these tests.

Iron ore pellets that have been exposed to high static stress or high falls, that can occur during filling of the silos, are not showing any decrease in LTD.

2.2 The silos

One part of classical silo design is the fundamentals of the flow profile. There are two main profiles called mass flow and funnel flow. Mass flow is defined as movement of the entire bulk in the silo, while the funnel flow is defined as when only the central part of the bulk is in motion. Illustrated to the left in Figure 2.3.

To the right in Figure 2.3 there is a classical diagram showing where mass flow and funnel flow respectively occur in a conical hopper, depending on different parameters.

The diagram does not consider the ratio between radius in the outlet and the bin, which is assumed to affect the flow pattern.

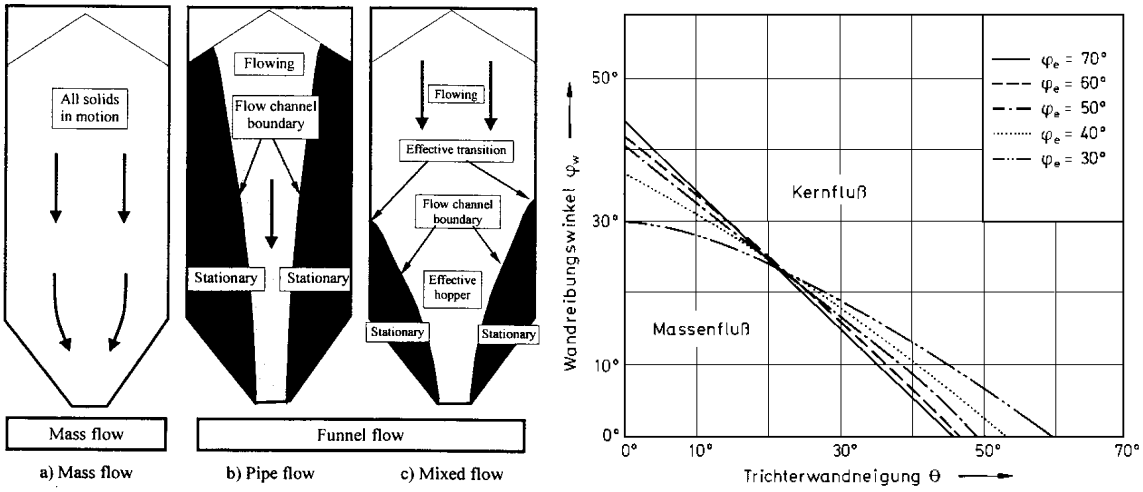

Figure 2.3: *Left: Basic flow pattern and definitions [1]. Right: Guiding diagram for flow profiles in a conical hopper as function of the internal friction, ϕ_e, the wall friction angle, ϕ_w, and the hopper angle, θ, [8].*

The design of the silo set by LKAB is 38 meters wide and about 65 meters high. The drawings from this original design can be found in Appendix A, where it also can be seen that the silo has a perforated inner tube. It is made of concrete and its inner diameter is 10 meters and its height is 47 meters. A model of the silo is presented in Figure 2.4. The inner tube is thought to induce a pipe flow that will guarantee traceability and low stress in pellets during movement. If it works well the pellets will discharge mainly from the upper level of the openings trough the inner tube.

2.3 The thesis

The simulations in this thesis are performed with ABAQUS/Explicit at the Center for Scientific and Technical computing, LUNARC, at Lund University. LUNARC provides large computer clusters which make it possible to run parallel jobs. This saves a large amount of time.

According to Figure 2.3, the flow pattern that can be expected is mass flow or funnel flow. A mass flow inside the inner tube would be the most logical result, as it makes the flow in the whole silo a pipe flow. Pipe flow is associated with lower stresses than mass flow. A funnel flow inside the inner tube would make the situation complicated. The existence could cause a situation where the flow has a smaller radius than the inner tube itself. If that condition is fulfilled, it would not be obvious that all pellets in the tube are involved in the movement. This would, besides what the stress condition is, perhaps ruin the traceability criterion if pellets inside the inner tube are mixed.

The modified designs are performed to seek solutions that better fulfill the traceability

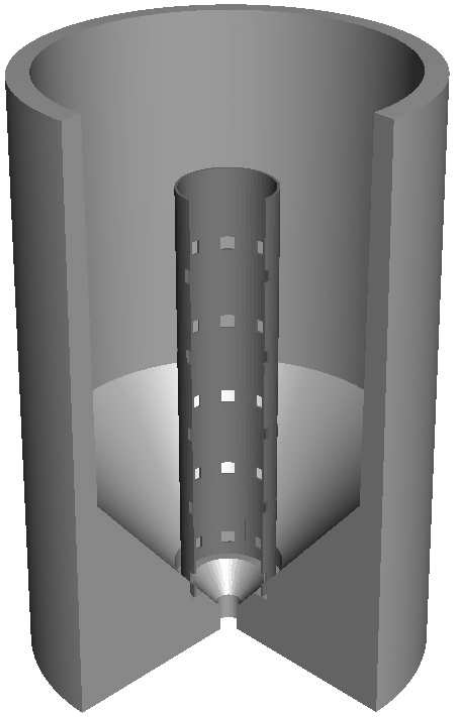

Figure 2.4: *A 270° model of a silo.*

criterion and lowers the stresses. The changeable parameters are the design geometrics and the texture of surfaces by using different materials.

The hopper angle can be changed, the walls of the hopper can be covered with steel plates instead of just blasted bedrock in order to change the friction coefficient. At the bottom of the tube there is a plateau for the scaffold that will be used during construction. It is possible to make this plateau oblique.

The inner tube will be casted with a thicker wall at the bottom than at the top. This can be used to make an oblique or indented stepwise inner side of the tube. The tube itself does not have to be as tall as in the original design.

The material parameters of the pellets are not possible to change in reality, but they might have theoretical uncertainties that are of interest to investigate. The parameters can affect the flow and the stresses in the result.

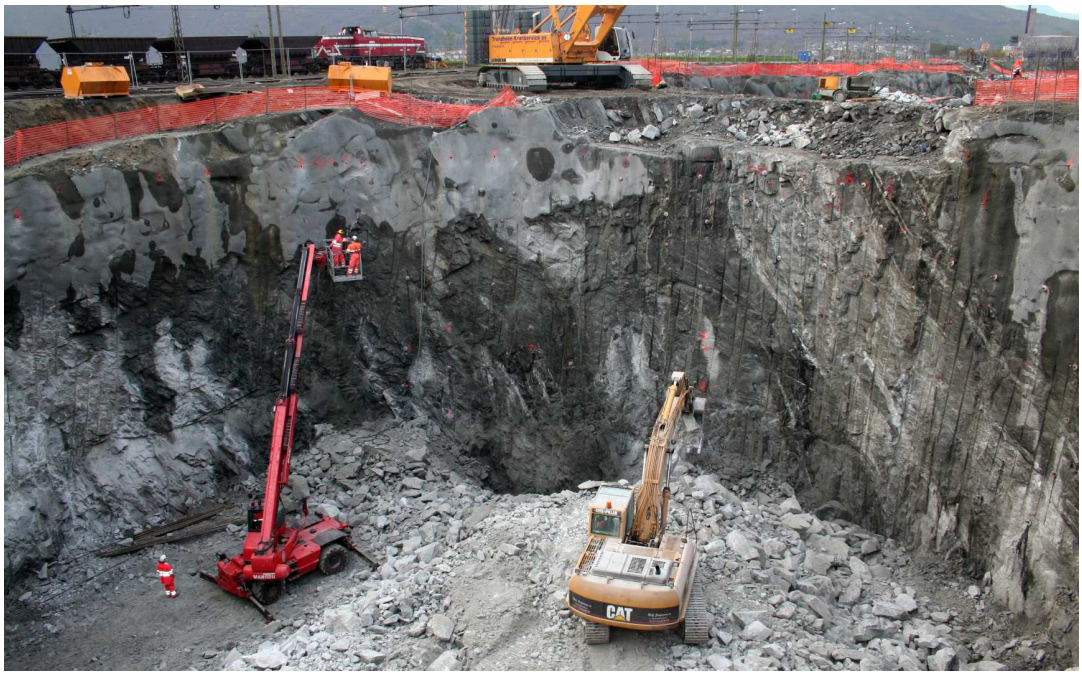

Figure 2.5: *Picture from the site showing the interior of a silo. Photo taken the 13th of October 2006. Image courtesy LKAB.*

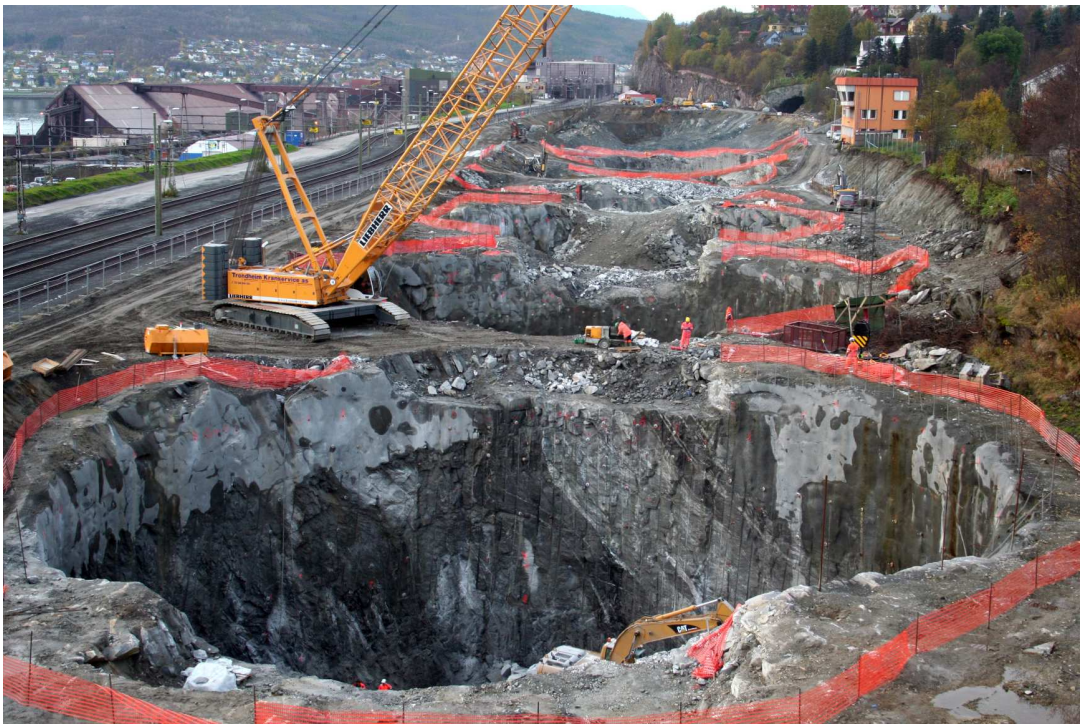

Figure 2.6: *Picture from the site showing the silos in row. Photo taken the 13th of October 2006. Image courtesy LKAB.*

Part II

Theory and methodology

Chapter 3

Finite element formulation

Finite element analysis are Lagrangian, which means that the mesh follows the material in its movement. If the material has a movement that is comparable to a flow, but without for that sake being a pure fluid like in a silo with granular matter, it will have large deformations and the mesh will suffer of severe distortion. This can be handled by an adaptivity mesh technique, which recalculates and optimizes the mesh by certain criterions during the analysis.

In a silo the Lagrangian description is suitable in the bin and at the upper free surface. At the outflow, where the material leaves the silo, the Eulerian is more suitable because then material can leave the mesh. The Eulerian description has a mesh that is fixed in space. This calls for an Arbitrary Lagrangian Eulerian, ALE, description of the problem where the two types of analysis can be combined.

If the silo has inserts, which the flow has to pass, the Lagrangian description of the mesh inside the bin will then again suffer from difficulties. As the upper surface of the material moves downwards, the mesh will be compressed above the insert. The only available solution is then the pure Eulerian description with the disadvantage that it must have a fixed upper surface with an inflow, to make sure no element lacks material. Hence, only steady states can be evaluated.

An illustration of the pure Lagrangian, the Arbitrary Lagrangian Eulerian (ALE) and the pure Eulerian description is available in Figure 3.1.

3.1 Analysis type

There are two different algorithms to solve a dynamic finite element problem, implicit and explicit. The implicit algorithm solves the equations of motion through the sets of coupled differential equations, in the mass and stiffness matrices, simultaneously. It is usually unconditionally stable and has no time increment size limit. However it is computational expensive to invert matrices and it may require many iterations to converge.

The implicit algorithm in ABAQUS uses the Hilber-Hughes-Taylor operator for integration, which is an extension of the trapezoidal rule. The solution is then iterated to con-

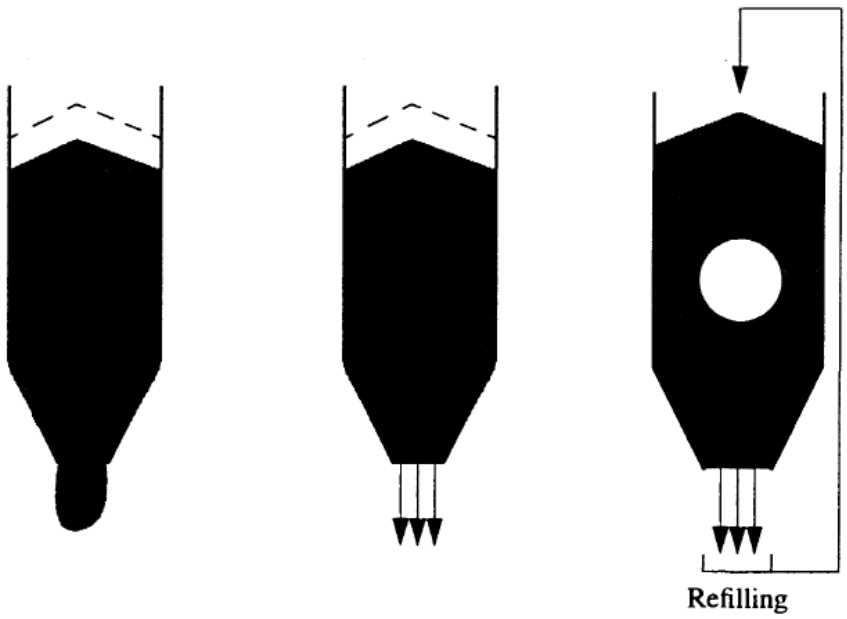

Figure 3.1: *From left: The pure Lagrangian, the Arbitrary Lagrangian Eulerian (ALE) and the pure Eulerian description. Original drawing from [5].*

vergence using Newton's method [2].

In the explicit algorithm, calculations are executed in terms of known quantities. Therefore there is no need for forming or inverting of the global mass and stiffness matrices. No equations have to be solved simultaneously. Each increment is computational inexpensive, although the size of the time increment is affecting the stability. An explicit method may contain a very large quantity of increments, generally of order 10000 to 1000000. ABAQUS uses a central difference method which is only conditionally stable.

The explicit solving method shows advantages in solving high-speed dynamic problems where the modelled time needed is in size with the stable increment. The tracking of wave propagation is important to capture the dynamic response. Stress waves of the highest frequency of the system may require very small time increment. Explicit methods have more advantages in handling complex contact problems, highly nonlinear problems and material with degradation and failure, where it can be difficult for an implicit method to converge.

It is far from obvious which method to use, even though choosing the explicit method has a computational cost advantage for very large problems -as in the current. The cost grows linear for a explicit method, compared to implicit methods, where it grows more rapidly than linear. This i illustrated in Figure 3.2.

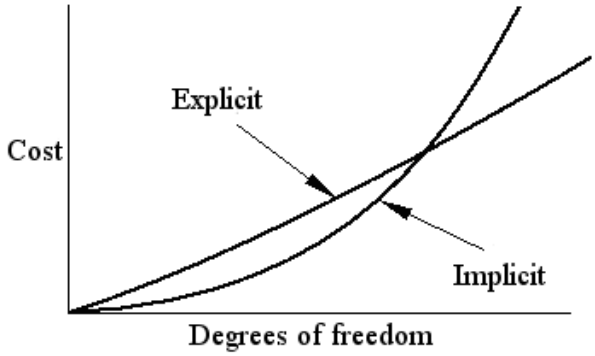

Figure 3.2: *Illustration of the computational cost versus degrees of freedom using explicit or implicit algorithms [3].*

3.2 Stability and increment time

The central difference method used in ABAQUS/Explicit is as mentioned conditionally stable. The stability limit, Δt, is given in terms of the highest rotational frequency, ω_{max}, of the system and is without damping given by

$$\Delta t \leq \frac{2}{\omega_{max}} \tag{3.1}$$

With damping expressed as the fraction of critical damping, ξ_{max}, in the mode with the highest frequency, the stability limit takes the form of

$$\Delta t \leq \frac{2}{\omega_{max}}(\sqrt{1+\xi_{max}^2} - \xi_{max}) \tag{3.2}$$

Damping in a small amount is always introduced by default in ABAQUS, to control high frequency oscillations.

An approximation of the stability limit, that will not require the computation of the highest frequency, is the smallest time it takes for a dilatational wave to transit the shortest element. With the smallest element dimension denoted as L_{min} and c_d as the dilatational wave speed the approximation becomes

$$\Delta t \approx \frac{L_{min}}{c_d} \tag{3.3}$$

3.3 Adaptive mesh generation

The chosen adaptivity mesh generating technique is the arbitrary Lagrangian Eulerian, ALE, method. The method introduces additional so called advective terms in the momentum balance and the mass conservation equations. The terms accounts for the independent

mesh and material motion where the modified equations can be solved directly or by an operator split that decouples the material motion from the additional mesh motion. The operator split is used in ABAQUS/Explicit since it is computationally efficient [2].

In every adaptive increment the whole model is first handled in a pure lagrangian manner. The solution is then remapped to the new mesh which is preformed by mesh sweeps under certain criterions.

3.3.1 Tracer particle

There is a possibility to track the time history of specific nodes during the simulations by the tracer particle function in ABAQUS. Every time an adaptivity increment is remapping the mesh, it calculates the new position of an earlier defined node that completely follows the physical matter.

The tracer particle can show movement, that is separated from vibrations, which are difficult to observe in an Eulerian simulation where the mesh is fixed in space.

3.4 Quad element with reduced integration

The only possible elements to choose in ABAQUS, when performing an analysis using an ALE adaptive mesh domain, are first order elements with reduced integration. In the explicit analysis the only element available that fulfills the conditions is the 8-node hexahedral element C3D8R. See Figure 3.3 for its definitions.

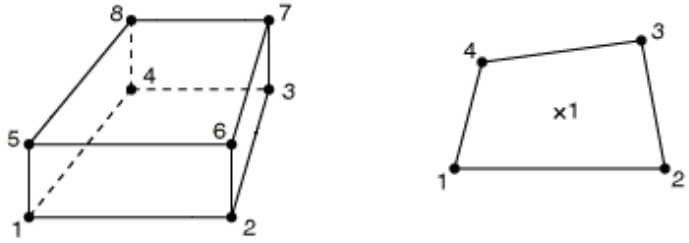

Figure 3.3: *The element C3D8R, with its reduced integration point, x1, [2].*

As the element only has one integration point it has problems with hourglassing. ABAQUS provides a function called hourglass control, but it is still recommended to use the element with a reasonably fine mesh.

Chapter 4

Constitutive relations

Granular matter, as iron ore pellets, has a constitutive relation that depends on the normal stress to a specific surface, and will without cohesion not resist any tensile stress. At a certain state of stress the material will yield. The material will undergo deformations until the stress state is beneath the yield criterion, also called the failure model.

Granular material usually consolidates when exposed to long time stress. The bulk density and shear strength increases as the particles become more tightly packed. When the material is exposed to deformation it will dilate, causing changes in the bulk density. Previous work of Karlsson [5] made the assumption that granular matter has constant bulk density as long as it is in motion.

In the simulation of flowing granular matter the initial consolidation is not taken into account. Therefore the bulk density can be taken as constant. The material is non-dilatant, and iron ore pellets have no cohesion.

4.1 Mohr-Coulomb plasticity

According to Mohr-Coulomb, failure occurs when the shear stress reaches a particular value that depends on the stress state which can be evaluated with Mohr's circle. The circles are drawn in the plane of minimum and maximum principal stress, σ_1 and σ_3. The failure line describing the limit is linear and touches the circles as in Figure 4.1 where c is the cohesion and ϕ is the angle of internal friction.

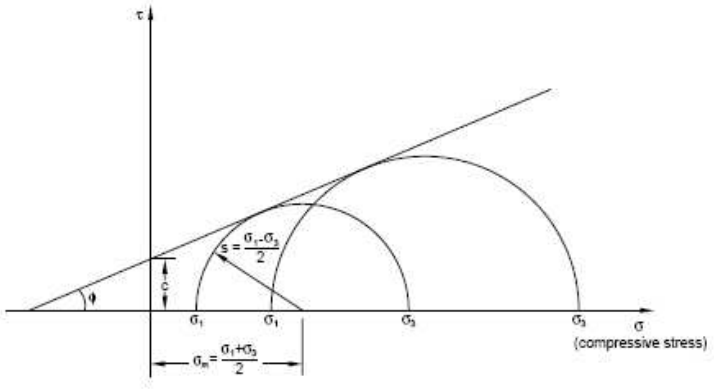

Figure 4.1: *Mohr-Coulomb failure model in two dimensions [2].*

The Mohr-Coulomb failure model takes no account to the third, intermediate principal stress. The discarding effect is small in most geotechnical materials and makes the Mohr-Coulomb criterion accurate for most applications [2].

The appearance of the Mohr-Coulomb model in the deviatoric plane is shown in 4.2. The discontinuing mathematical behavior can be somewhat difficult to handle numerically. A smoother constitutive law is the Drucker-Prager model that will also account for all principal stresses.

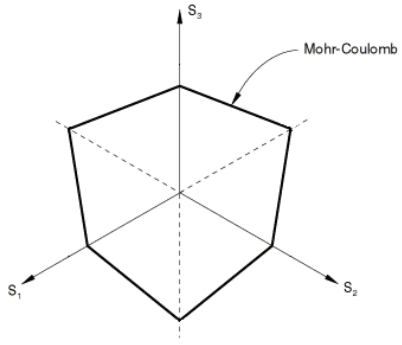

Figure 4.2: *Mohr-Coulomb failure model in the deviatoric plane [2].*

4.2 Drucker-Prager plasticity

The Drucker-Prager model takes account for all principal stresses. In its most generic form, the criterion is stated in terms of the first stress invariant I_1 and the second stress deviator invariant J_2 as [7]

$$F(I_1, J_2) = 0 \tag{4.1}$$

where

$$I_1 = \sigma_{ii} \tag{4.2}$$

$$I_2 = \frac{1}{2}\sigma_{ij}\sigma_{ji} \tag{4.3}$$

$$J_2 = I_2 - \frac{1}{6}I_1^2 \tag{4.4}$$

The explicit and linear form of (4.1) for a nondilatant material is a relation between I_1 and $\sqrt{J_2}$ stated in

$$F = q - p\ tan(\beta) - d = 0 \tag{4.5}$$

where q is the equivalent von Mises stress

$$q = \sqrt{3J_2} \tag{4.6}$$

and p is the equivalent pressure stress, also named hydrostatic stress or just pressure.

$$p = -\frac{1}{3}I_1 \tag{4.7}$$

The illustration of the yield surface in the $p - q$ stress plane, or the meridional plane is seen in Figure 4.3. Included is the interpretation of the cohesion d and the frictional angle β of the material.

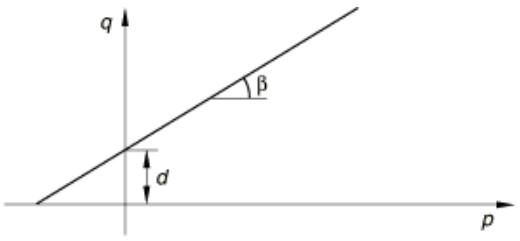

Figure 4.3: *The linear Drucker-Prager yield surface in the meridional plane [2].*

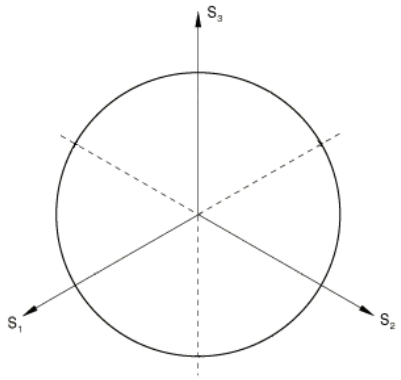

Figure 4.4: *The Drucker-Prager model in the deviatoric plane [2].*

The relation between the parameters of the Mohr-Coulomb model and the Drucker-Prager model is for triaxial compression and tension with nondilatant flow:

$$tan(\beta) = \frac{6sin\phi}{3 - sin\phi} \tag{4.8}$$

4.3 Frictional contact

Where two surfaces meet, there has to be a constitutive relation to be able to handle the physical characteristics numerically. In general there is one normal and one tangential property to the surface that transmit normal and shear force respectively.

The shear stress is often proportional to the contact pressure, p, as in the theory of Coulomb friction where the critical shear stress between two surfaces is

$$\tau_{critical} = \mu p \tag{4.9}$$

If the shear stress exceeds $\tau_{critical}$, then the surfaces will slide relative to each other.

There are different types of algorithms to calculate the contact pressure. One is the Kinematic contact algorithm which is a predictor/corretor algorithm. Every increment is first calculated by neglecting the contact relations and allows for one of the surfaces to penetrate the other. This predictor step calculates then the node forces required to oppose this penetration into the other surface by the use of penetration depth, the associated mass and the incremental time. The corrector step then evaluates the data depending on the surfaces properties, whether they are deformable or discrete.

Chapter 5

Simulation conditions

As the simulation has to be performed with an Eulerian description, the time history data of the discharge cannot be captured. Even if it were possible to simulate the upper surface with a Lagrangian description, the physical discharge time is as long as 13 hours and would be impractical to calculate. Therefore the simulations have to be done at specific states. The states can be found by evaluating and discuss the result of the previous simulated states.

The forces acting on the pellets are gravitational and frictional forces. The gravitational force will cause a compaction of the pellets immediately when the simulation begins and will disturb the location of the tracer particles with an unnatural movement. Therefore the simulation needs a first step, where the compaction is simulated, and thereafter a second step where the outlet will be opened. The first step also gives the static stress condition. To avoid unwished transients the applying of the gravity force and the opening of the outlet should be simulated smoothly.

5.1 Density

The density of interest for modelling the pellets as a continuum is the bulk density which is 2300 kg/m^3.

5.2 Elasticity

The elasticity module and the lateral contraction ratio is ambiguous. In the work of Gustafsson [4] it is indicated that both the modulus of elasticity and the Poissont's ratio depend on the stress state, however the dependency is not fully investigated. The values are then set to consist of average values from the current work.

The simulations will have an elastic modulus of 2.4 MPa and a Poisson's ratio of 0.4.

5.3 Plasticity

The plasticity part in the constitutive relation is described by the Drucker-Prager failure model. The angle of internal friction is assumed equal to the angle of repose evaluated by [6]. The angle of repose is found to be about 26°, which is also claimed in the European Standard [1]. The European Standard is also claiming that the angle of internal friction is somewhat higher than the angle of repose, about 31°.

If the angle of 26° is assumed to be the internal friction of the Mohr-Coulomb failure model, ϕ, it is needed to be recalculated to obtain the angle of internal friction of the Drucker-Prager failure model, β as

$$\beta = tan^{-1}\left(\frac{6sin26}{3 - sin26}\right) = 46 \tag{5.1}$$

It is the same value as Gustafsson [4] found, and is therefore settled as the most interesting value. But it is still of interest to simulate how eventual fluctuations, in the angle of internal friction, will influence on the stresses and the flow pattern in the silo.

5.4 Friction

The friction is a property with large impact on the result. The lower the friction is, the higher the stresses will be in the pellets. More force will be received in the bottom of the silo where more horizontal surfaces exist. If the material fails along the walls, higher friction coefficients will have no impact on the stresses.

The friction coefficients, between iron ore pellets and the walls, is found in the European Standard [1]. The values are formulated as an average value and a modification coefficient to give upper and lower characteristic values.

For a wall type D2, which is defined as steel finished concrete and carbon steel with light surface rust, the average value is $\mu = 0.54$ with upper characteristic value of 0.6 and lower of 0.48. For a wall type D3, which is defined as off-form concrete, the average value is 0.59 with upper characteristic value of 0.66 and lower of 0.53.

The inner tube will be made of off-form concrete and the silo walls of blasted bedrock. The inner tube is of a wall type D3, however the walls of bedrock are harder to evaluate. As pellets in the outer part of the silo are expected to be in a static condition, the friction coefficient are not that important as inside the inner tube. In the hopper, located inside the inner tube, the pellets will move and the friction coefficient is therefore important. The hopper can be covered by steel plates to give low friction coefficients and is in that case a wall of type D2. Otherwise the friction coefficient is assumed to be ”high”.

It is of interest to simulate how larger fluctuations of the friction coefficient will affect the stresses and the flow pattern.

5.5 Boundaries

The drawings of the original design of the silo are presented in Appendix A. From the drawings it can be found that the silo has a symmetry of 22.5°. The use of symmetry in simulations is a very efficient way to reduce the computational cost. The representative model of the silo with the inner tube and the bedrock is shown in Figure 5.1.

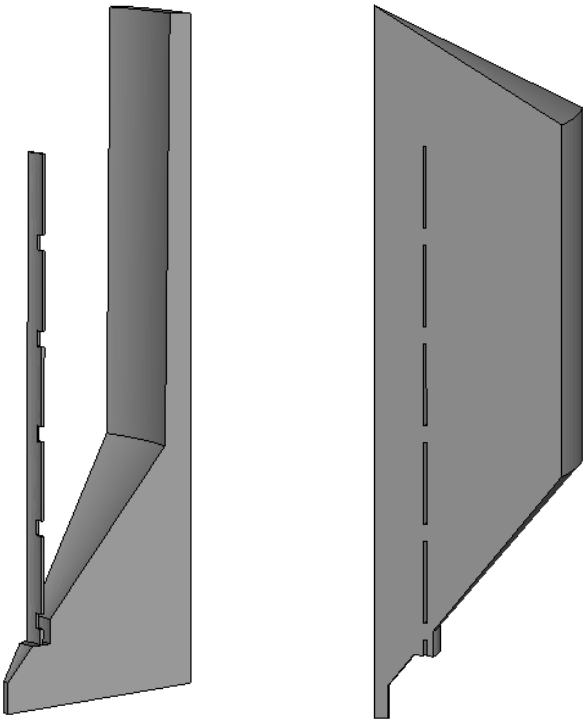

Figure 5.1: *The representative model of the silo with the inner tube and the bedrock separated from the pellets with the appearance of a full silo.*

The appropriate boundary condition at the outlet is the velocity of the pellets. The discharge will be done with a mass flow of 10 000 tons per hour. The outlet has the geometry of a circle with a 2.7 meter diameter.

With the density of 2300 kg/m^3 the volume flow Q of the pellets will be

$$Q = \frac{10000}{2.3 \cdot 3600} = 1.208 m^3/s \tag{5.2}$$

and the velocity v given by

$$v = \frac{1.208}{1.35^2 \pi} = 0.2108 m/s \tag{5.3}$$

The boundary conditions at the symmetry sides of the pellets will be expressed in cylindrical coordinates with a prescribed zero velocity in the angular direction. It is usually done with displacements, but as the outlet has got a boundary condition expressed as

prescribed velocity, it will cause difficulties at the edges that are separating two surfaces with different types of boundary conditions.

The vertical line in the center of the model will have a prescribed velocity of zero in the radial direction in a cylindrical coordinate system. The reason to describe the condition as prescribed velocity is the same as for the symmetry sides.

The inlet at the upper surface will have no boundary condition, more than the mesh constraint, that makes the mesh domain Eulerian. Material will be free to flow across the surface and ”fill” the mesh as the silo discharges. During the first step, when the compaction is simulated, it will be possible to see if the assumed surface in the current state is stable. If it is not, there will be a flow indication.

5.6 Stresses and strain

The limit of 250 kPa vertical stress is evaluated from tests made inside a rubber cylinder with an axial load and a horizontal displacement between the upper and lower circular surfaces. The vertical stress limit is taken from the axial load with a good margin. As the shear stress state in the cylinder is not known, it could be of interest to evaluate not only the vertical stresses but also the principal stress.

Equivalent plastic strain or PEEQ, is an interesting parameter that can show where the material has plastic strain. The plastic strain indicates yield surfaces that can be of interest in the analysis. It is defined by

$$PEEQ = \int_0^t \dot{\epsilon}^{pl} dt \tag{5.4}$$

Where $\dot{\epsilon}^{pl}$ is the strain rate in uniaxial compression.

Part III

Result

Chapter 6

Original design

This chapter evaluates the silo in its original design, as it is established by LKAB in collaboration with specialists on the subject. Experimental scale tests on silos both with and without an inner tube are done as a part of the design process.

There are mainly two reasons of having an inner tube. At first it is thought that it reduces the stresses in the pellets by reducing movement to inside the tube. The second reason is that if the pellets are mostly discharging through the upper opening, while having a uniform velocity inside the tube, then it is possible to have almost full control over the traceability. This will produce an artificial pipe flow.

By first looking at the classical silo design, shown in Figure 2.3, with a friction coefficient of about 0.5, with the internal friction of the pellets set to 26° and with a slope in the hopper of 40°, a funnel flow could be expected. This will ruin the traceability criterion if the bulk inside the tube is mixed.

The angle of the hopper will have to be as precipitous as 20° or the friction coefficient has to be reduced to 0.2 to give a mass flow inside the inner tube. The diagram assumes a perfect silo. The original design also has a plateau at the transition between the inner tube and the hopper. The plateau is for supporting scaffolding during construction.

In terms of stress, a high friction coefficient will give low stresses in the pellets but high forces on the structure. In terms of flow pattern, high friction coefficients will tend to make the flow a funnel flow inside the inner tube and low friction coefficients will tend the flow to become a mass flow.

The characteristics of the influence from the friction coefficient is therefore complex. Higher as well as lower coefficients are of interest since low coefficients give high stresses while high coefficients give the presumed unwished funnel flow.

The upper bound of the friction coefficient is used to evaluate the flow profile since it is preventing a mass flow. The lower bound is used to evaluate the stress condition. If there is mass flow, at high friction coefficients, there will also be a mass flow at low friction coefficients.

6.1 Discharge state 1

The discharge state 1, of the original silo, is a full silo containing about 50000 cubic meters or 110000 tons of pellets. The simulation is done with an overall friction coefficient set to 0.5. It is a lower boundary that evaluates the highest stress possible. The model has about 30000 elements and is executed until the flow stabilizes.

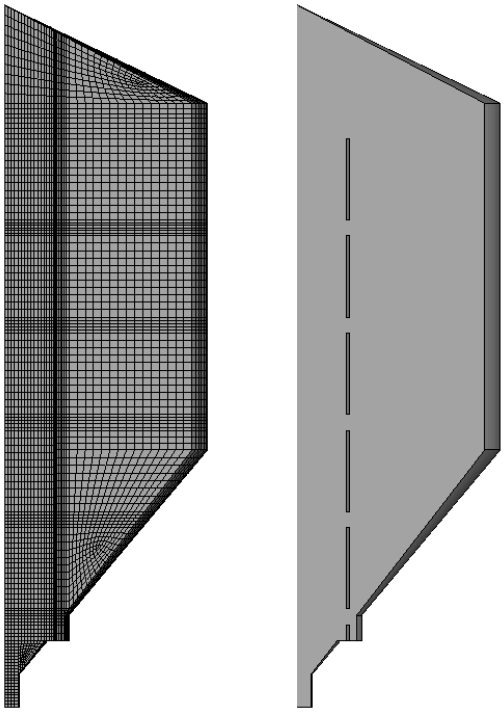

Figure 6.1: *The model of the pellets in the Discharge state 1 with and without the mesh.*

The vertical and the minimum principal stress distribution is shown in Figure 6.2. The figure shows that the stress distribution on the two sides are very alike. In the following figures only the side or view, that is of interest will be shown with a limited scale to 250 kPa, to clarify the stress distribution of interest. The maximum stress level and location is found in the text.

In Figure 6.3 is the equivalent plastic strain distribution, PEEQ distribution, presented together with vertical and minimum principal stresses on a limited scale. The figure shows a clear yield surface, in the PEEQ picture, which also has a characteristic appearance in the stress distribution.

The flow is a combination of pipe and mass flow, not to be mistaken with the mixed flow in Figure 2.3. The pipe flow develops from the outlet and upwards. As the pipe flow develops there is a pure mass flow in the tube. When the flow is fully developed the pellets inside the yield surface, the pipe flow have a high velocity. Outside the yield surface, the mass flow has a very low velocity but a much larger horizontal area. The flow outside the yield surface has a decreasing velocity further down in the tube, indicating that it is streaming through the yield surface towards the pipe flow.

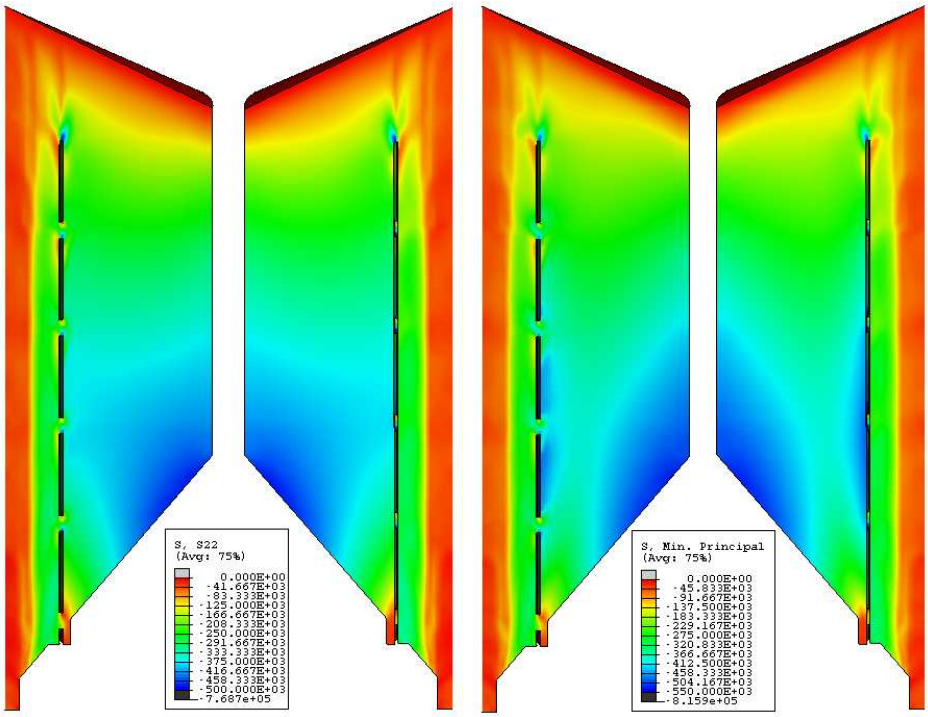

Figure 6.2: *Discharge state 1. Vertical and principal stress distribution on both sides.*

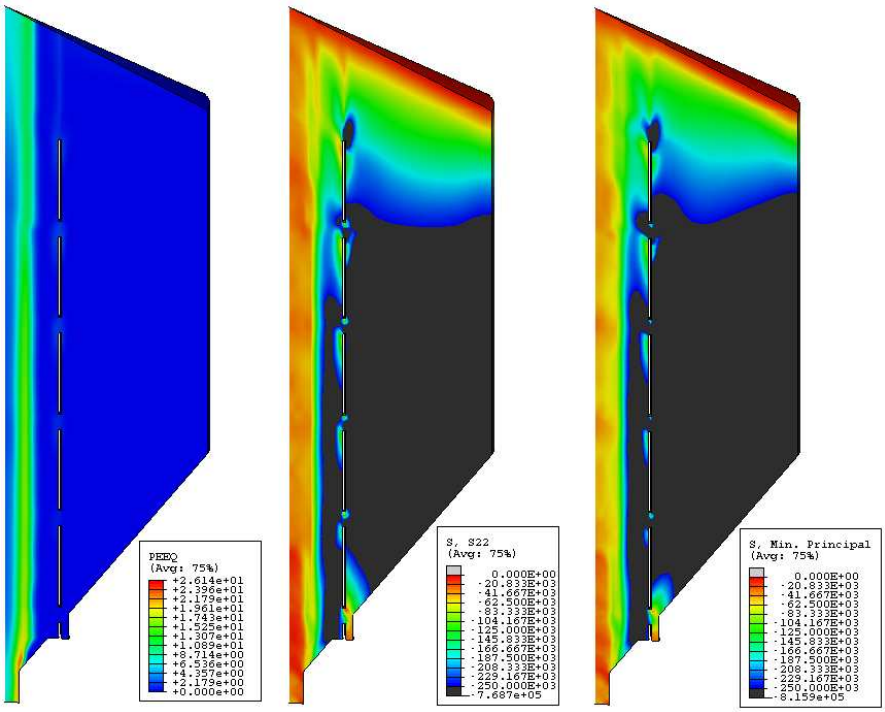

Figure 6.3: *Discharge state 1. PEEQ together with the vertical and principal stress distribution at a limited scale set to 250 kPa. Maximum vertical stress is 320 kPa above the plateau and principal stress is 370 kPa at the three upper openings.*

A calculation at the top of the inner tube shows that the pipe flow is around 1.1 m^3/s and the mass flow 0.1 m^3/s. A light yield surface can be seen above the top of the inner tube that is separating the mass flow from the surrounding pellets. Then the outflow consists up to 10% of pellets that have an uncertain origin. It is possible that they have had their way through with high stress areas.

The maximum vertical stress is 320 kPa and the maximum principal stress is as most 370 kPa, both located outside the yield surface in the mass flow. The highest vertical stress is located above the plateau, in the bottom of the inner tube and the highest principal stress is found at the openings. The vertical stress is influenced by the horizontal surface and the principal stress by shear stress from the opening's horizontal surface. The principal stress is highest at the three openings at the top where the velocity is higher than further down. There is no flow through the openings.

6.1.1 Impact of the friction coefficient μ

PEEQ and stresses obtained from simulations with a friction coefficient set to 0.6, 0.4 and 0.3 are shown in Figure 6.4, Figure 6.5 and Figure 6.6. The friction coefficient is the same for all contact surfaces. The model and the element used are as in the previous simulation.

At the two lower friction coefficients it is interesting to see if the silo develops a pure mass flow. The friction coefficient at 0.6 is interesting because it represents the average value of the friction against the wall of type D3 that the inner tube consists of.

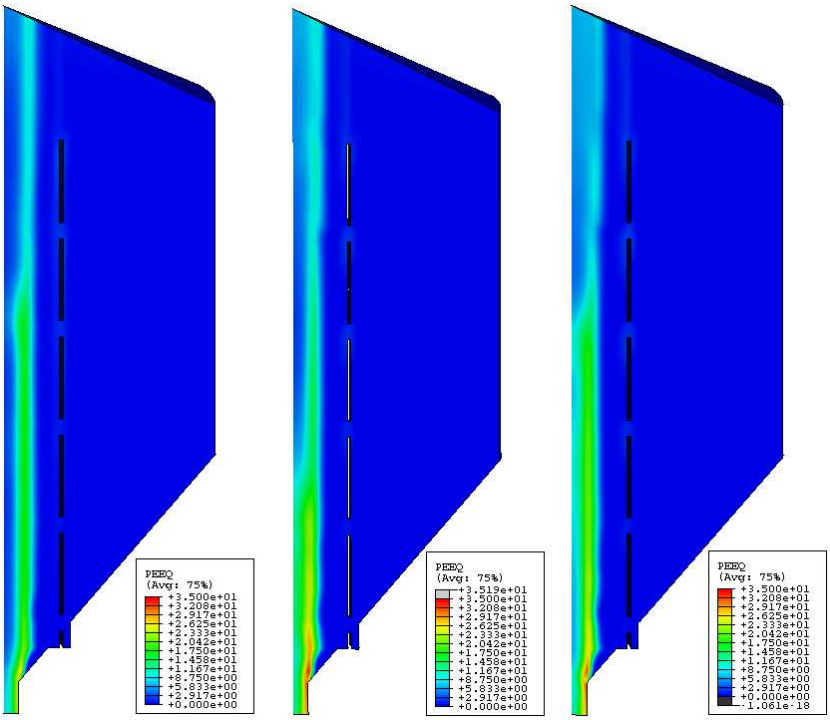

Figure 6.4: *PEEQ from simulations with a friction coefficient of 0.6, 0.4 and 0.3 respectively. The location of the yield surface is almost unaffected.*

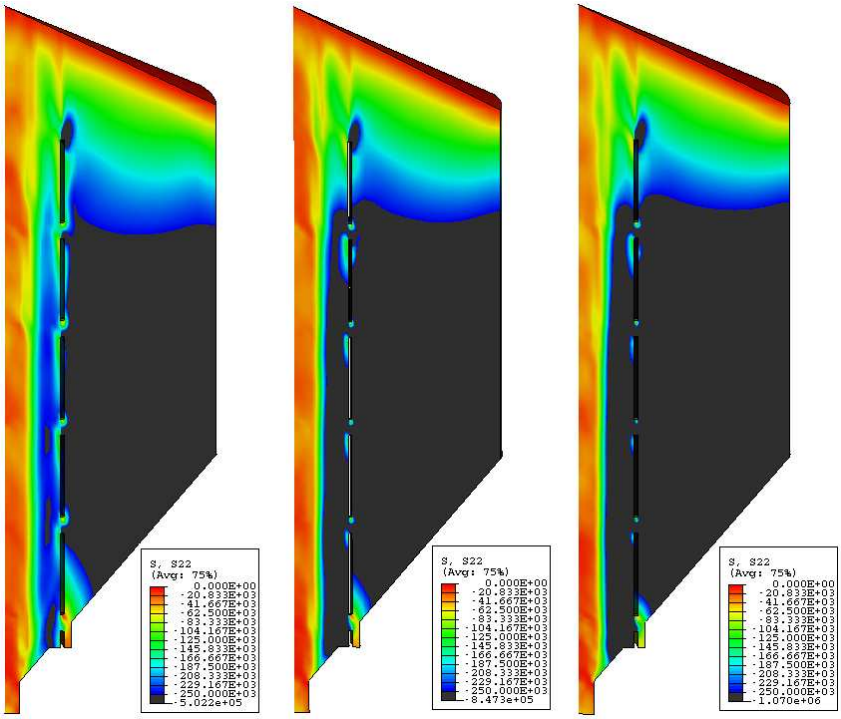

Figure 6.5: *Vertical stress obtained from simulations with a friction coefficient of 0.6, 0.4 and 0.3 respectively. Highest vertical stress is found above the plateau at 265 kPa.*

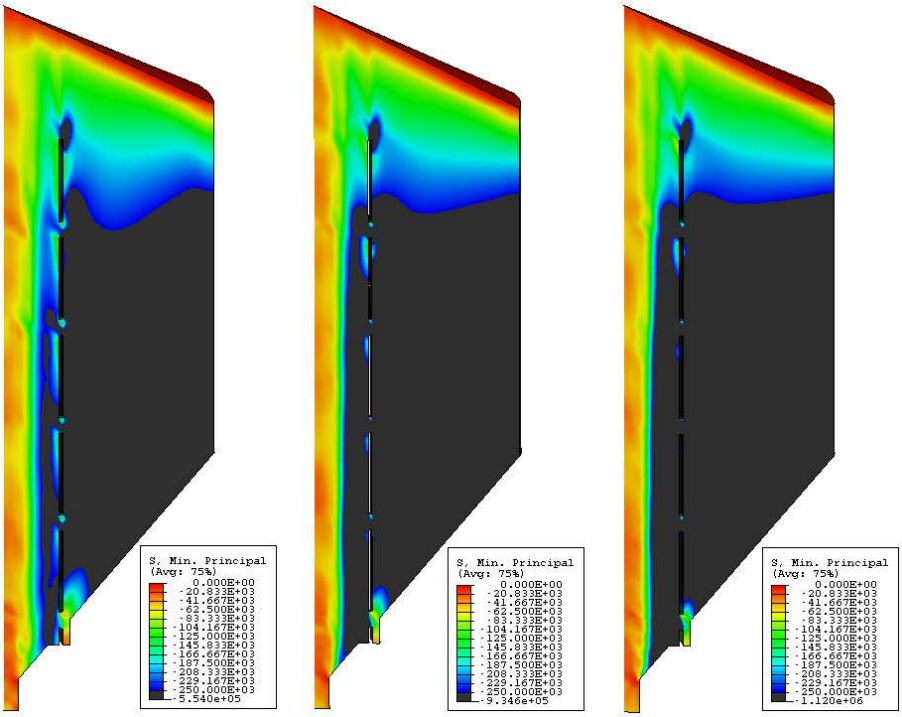

Figure 6.6: *Principal stress from simulations with a friction coefficient set to 0.6, 0.4 and 0.3 respectively. Highest principal stress is found at the intermediate opening at 280 kPa.*

The location of the yield surface and the flow pattern is almost unaffected by the changes. The silo has no tendency to develop a mass flow at these friction coefficients. The stresses are decreased when the friction is higher and are increased when the friction is lowered as it was assumed. At the friction coefficient 0.6 the maximum vertical stress is reduced to 265 kPa and the maximum principal stress to 280 kPa.

6.1.2 Impact of the material parameter β

The influence from fluctuations in the material parameter β, in the Drucker-Prager failure model, is of interest since it is not definite. The simulations, shown in Figure 6.7, 6.8 and 6.9, are done with the material parameter β set to 39°, 41°, 48° and 50° respectively and with the lower bound of the friction coefficient 0.5. It is shown that the yield surface is changed to approximately 40°. At 39° a pure mass flow is established. A Drucker-Prager parameter β set to 39° corresponds to a Mohr-Coulomb angle ϕ of 21° which is far from the current and is not realistic.

The stresses are increased at higher angles as seen in the figures. The stresses of $\beta = 50°$ are therefore interesting. If there are uncertainties in the material parameter the stresses can be influenced in a negative direction. The vertical stress is as most 370 kPa at $\beta = 50°$ compared to 320 kPa at the previous simulation with $\beta = 46°$. The European Standard [1] claims that iron ore pellets have an internal friction angle as high as 31°. That value corresponds to a Drucker-Prager angle of 52°.

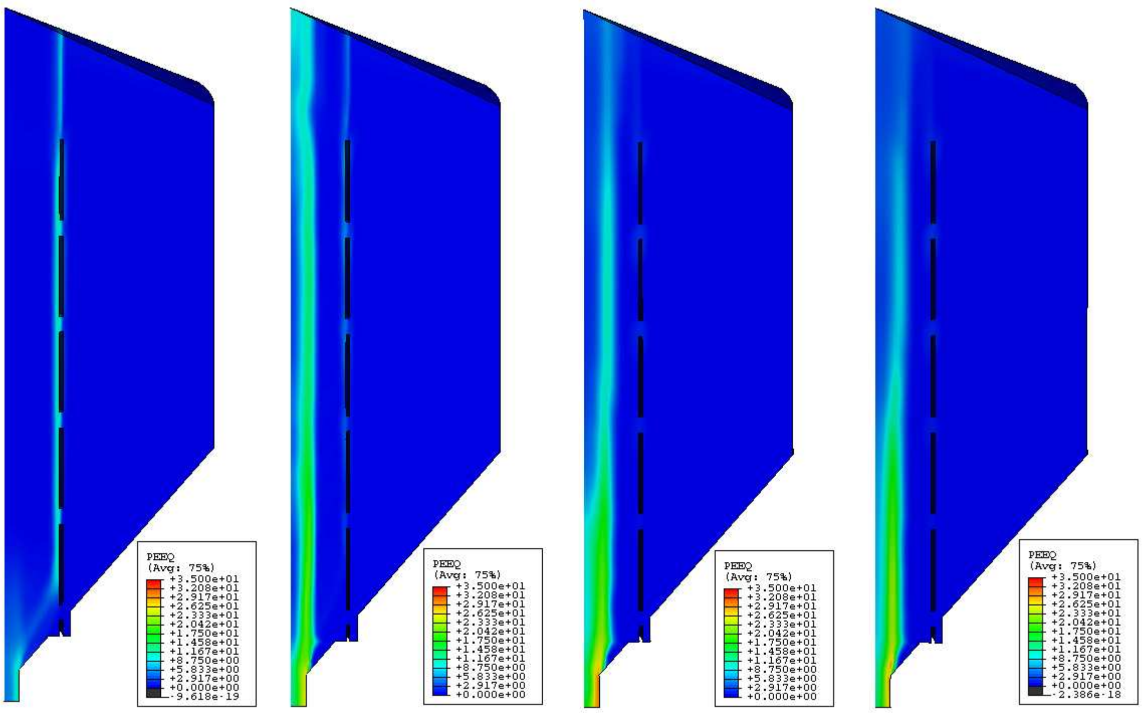

Figure 6.7: *PEEQ from simulations with β set to 39°, 41°, 48° and 50° respectively. At $\beta = 39°$ a pure mass is observed.*

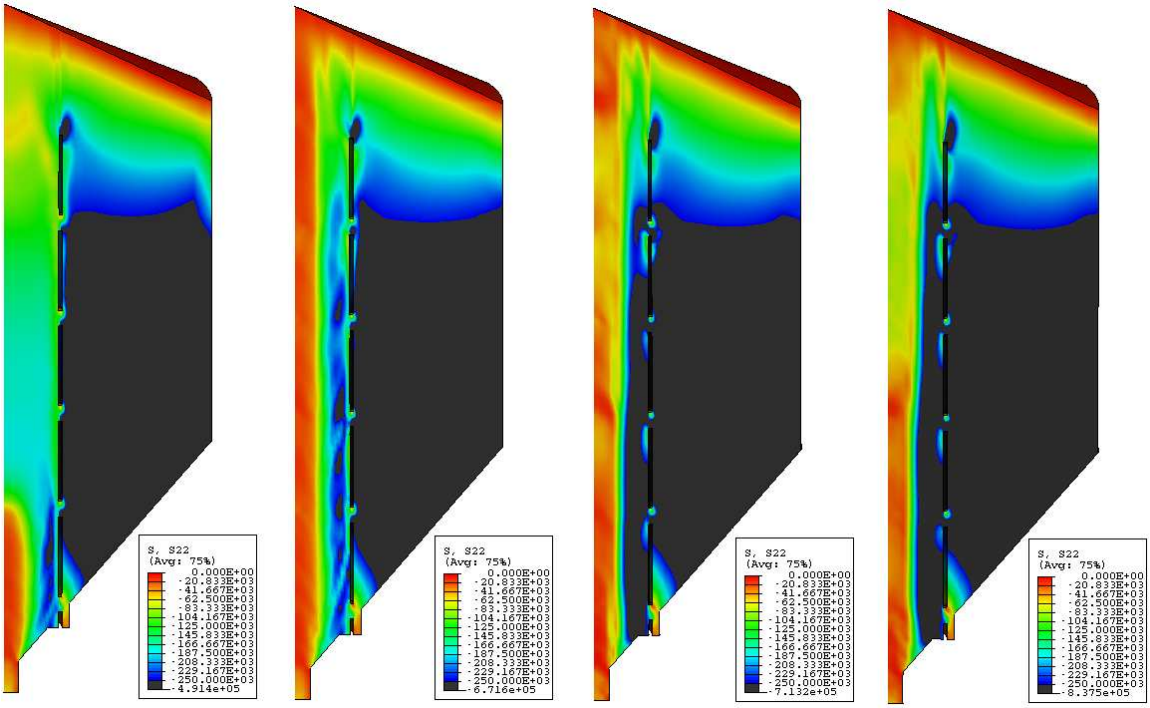

Figure 6.8: *Vertical stress from simulations with β set to* 39°, 41°, 48° *and* 50° *respectively. At* $\beta = 50°$ *the maximum stress is 370 kPa outside the second opening from the top.*

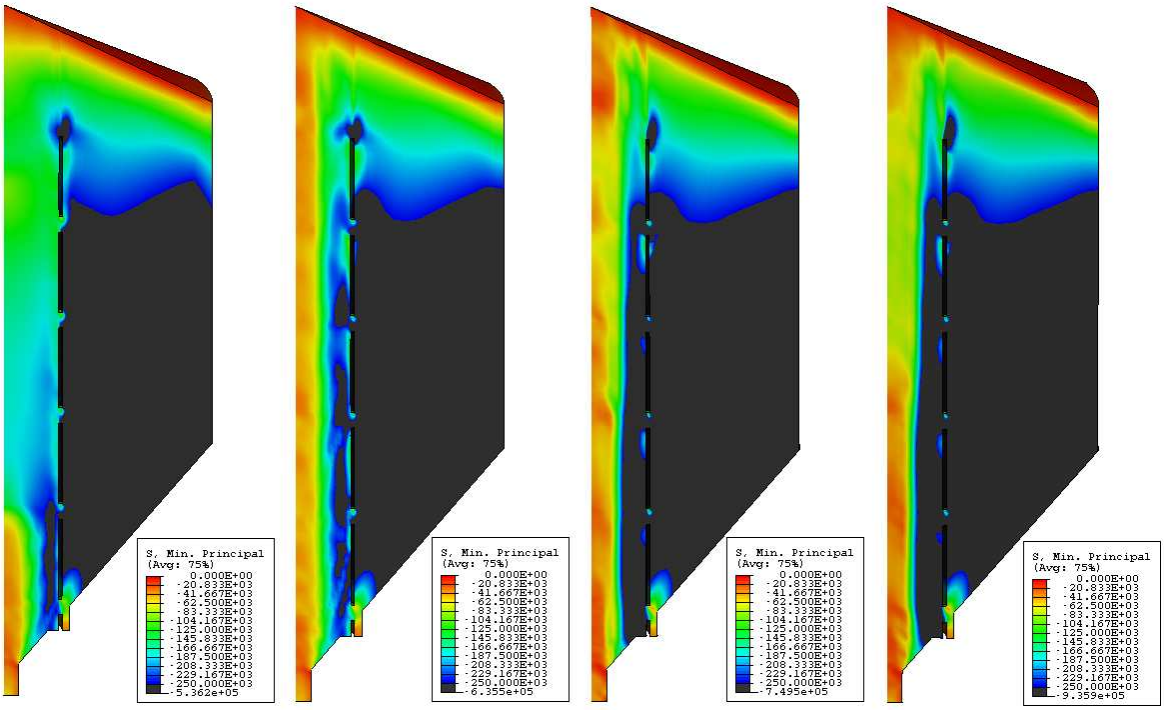

Figure 6.9: *Principal stress from β set to* 39°, 41°, 48° *and* 50° *respectively. At* $\beta = 50°$ *the maximum stress is 420 kPa outside the second opening from the top.*

6.2 Discharge state 2

The Discharge state 2 is defined as when the upper surface of the pellets reach the top of the inner tube. This is assumed to have the appearance of Figure 6.10 since the only flow indicated in Discharge state 1 is in the inner tube and above. The pellets, that are filling the pipe flow from the top, will form an avalanching surface as a cone; with oblique sides that are of the angle of repose at 26°. This should only be correct if there is flow inside the tube. The simulation is executed with an overall friction coefficient of 0.5. The state will appear approximately 65 minutes after the beginning of the discharge.

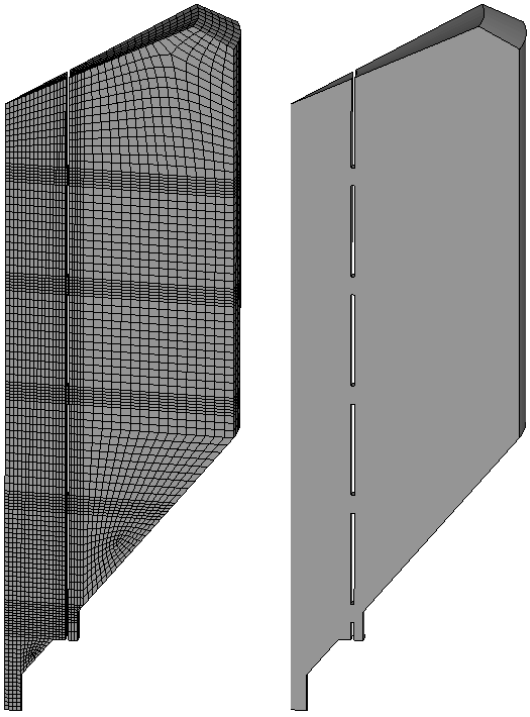

Figure 6.10: *The model of the pellets in the discharge state 2 with and without the mesh.*

The results, are presented in Figure 6.11 and 6.12, show that the flow is still a combination of a pipe and a mass flow. It is also found that there is still no flow in the openings, which strengthens the assumptions above about the appearance of the state.

It is also found that the yield surface is very alike the one in Discharge State 1 and that high pressures outside the pipe flow are still left. The maximum vertical stress is 305 kPa and maximum principal stress is 335 kPa.

6.3 Discharge state 3

Since the Discharge state 2 indicates that there is no flow in the upper opening in the inner tube, it can be assumed that the upper surface in the inner tube is lowering. At a

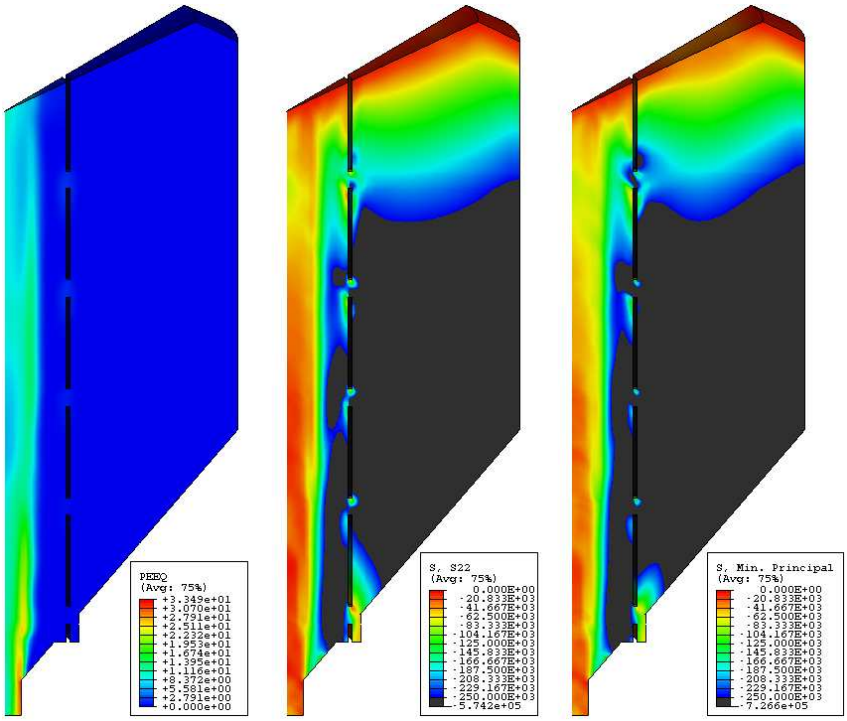

Figure 6.11: *Discharge state 2. Maximum vertical stress is 305 kPa and maximum principal is 335 kPa.*

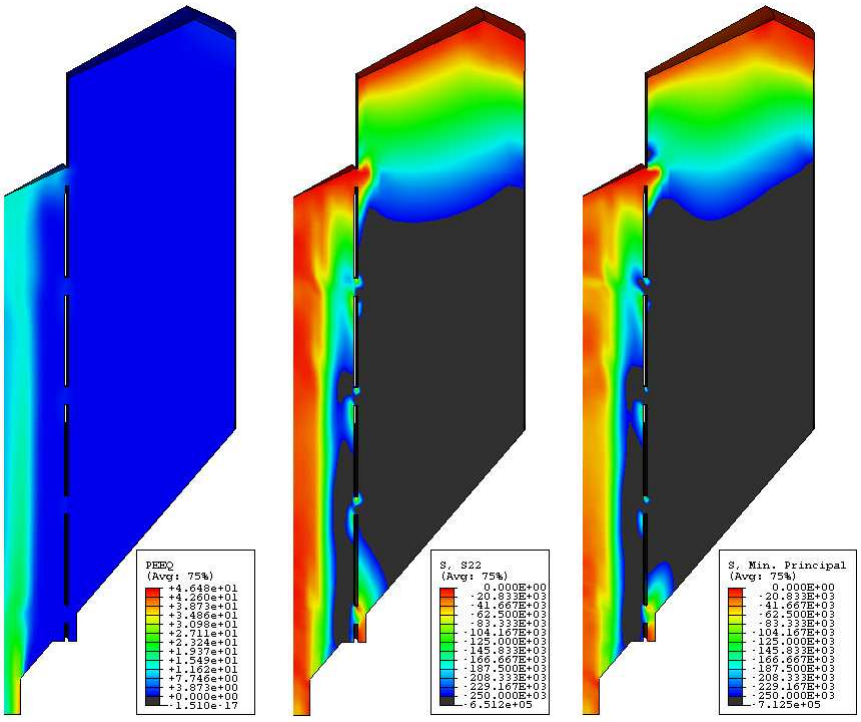

Figure 6.12: *Discharge state 3. Maximum vertical stress is 315 kPa and maximum principal is 350 kPa.*

certain level the pressure difference, at the opening, will be high enough to cause a flow through it.

The worst case, causing the highest pressure difference for the openings, should be if the surface in the tube will be at the upper side of an opening and the surface outside the tube, is at the lower side the opening above. The pressure difference could cause a flow at two openings simultaneously and ruin the traceability criterion. The appearance is called Discharge state 3 and is shown in Figure 6.13.

When the upper surface, inside the tube, reaches the upper side of an opening there will be a flow only through the opening. This is hard to simulate as it causes a difficult geometry inside the tube under influence of the angle of repose. Therefore the moment just before the opening is exposed will be simulated. The flow trough the upper opening is most likely going to be underestimated. But not the opening below, which is of most interest.

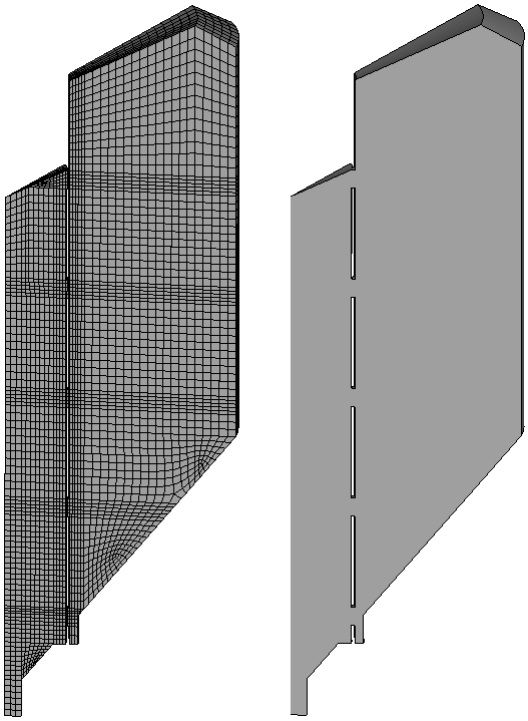

Figure 6.13: *The model of the pellets in the discharge state 3 with and without the mesh.*

The simulation shows that there is a flow through the upper opening but nowhere else. The yield surface and the stress distribution is showed in Figure 6.12. High stresses above the plateau in the bottom of the inner tube are still left and maximum vertical stress are 315 kPa and maximum principal stress are 350 kPa. The flow is still a combination of a pipe flow surrounded by a mass flow inside the tube.

Chapter 7

Modified design

With knowledge of the conditions in the original design of the silo it is of interest to investigate the effects of modified designs.

7.1 No inner tube

The simulations presented below evaluates the benefit of having an inner tube, and are carried out on the original design but without the tube and the foundation plateau. The model is shown in Figure 7.1. The first simulation is performed with a friction coefficient overall set to 0.5. The second simulation investigates the impact of a very rough bedrock and has a no slip condition at the interaction between pellets and the bedrock walls.

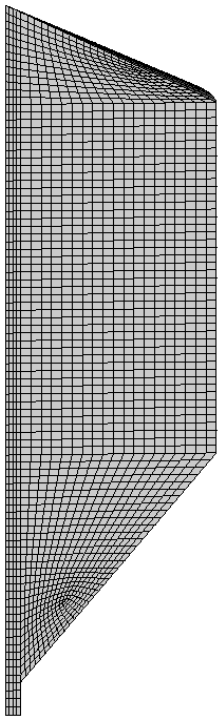

Figure 7.1: *The model of the pellets without an inner tube.*

In the simulation with the friction coefficient set to 0.5, pipe flow is fully developed after 500 seconds. The result can be found in Figure 7.2, showing only vertical stress. During the development there is pure mass flow in the whole silo as earlier, but very slow according to the large volume in relation to the volume in the inner tube. When pipe flow is fully developed the stresses are high just outside the transition zone and there is a very small movement even outside the pipe flow. However, the velocity is very small, only a few millimeters per minute.

According to the simulations the silo exceeds the stress limit as there is movement in areas with high stresses. Nor is the traceability criterion fulfilled, if the pellets are entering the pipe flow through the transition zone, and not only by avalanching at the upper surface towards the center. The result of the simulation, with the no slip condition, has little lower stresses and seems to develop the pipe flow faster than the simulation with the friction coefficient set to 0.5. The result is shown in Figure 7.3.

A question arises if the pellets in practice outside the pipe flow are stationary as in Figure 2.3 or not. Perhaps an experiment or a built full scale silo can show what.

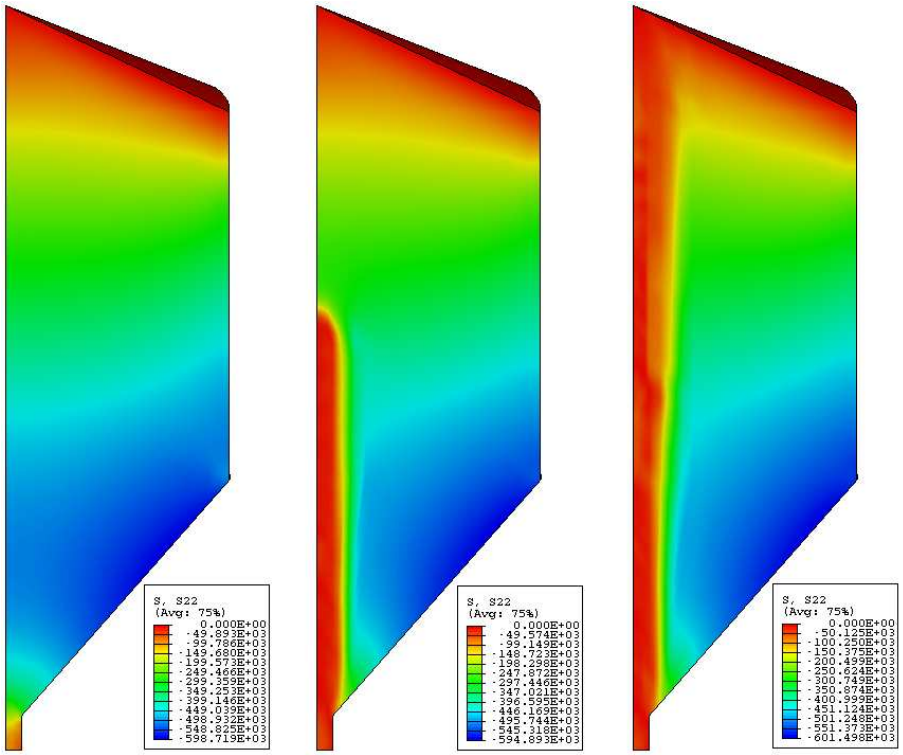

Figure 7.2: *The result with* $\mu = 0.5$ *at static condition, after 300 s and after 1200 s.*

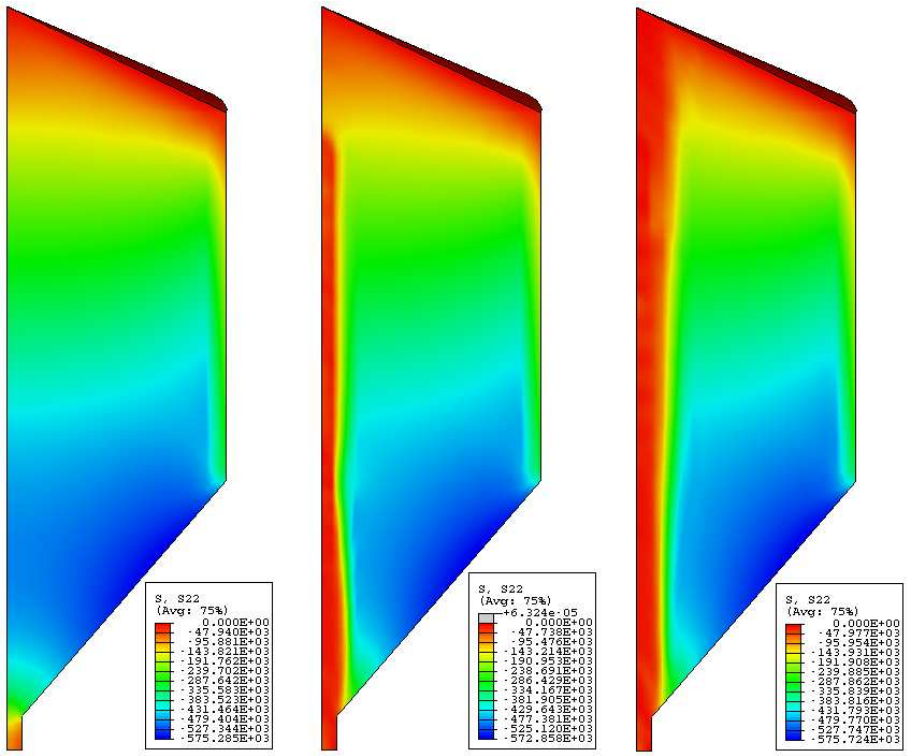

Figure 7.3: *The result with no slip along the walls at static conditions, after 300 s and after 1000 s.*

7.2 Design modification 1 - Oblique plateau

In the bottom of the inner tube there is a plateau for foundation and for scaffolds during the construction work. During the design process the possibility of making the plateau oblique afterwards was discussed. The model used in the simulation is shown in Figure 7.4 with an overall friction coefficient set to 0.5.

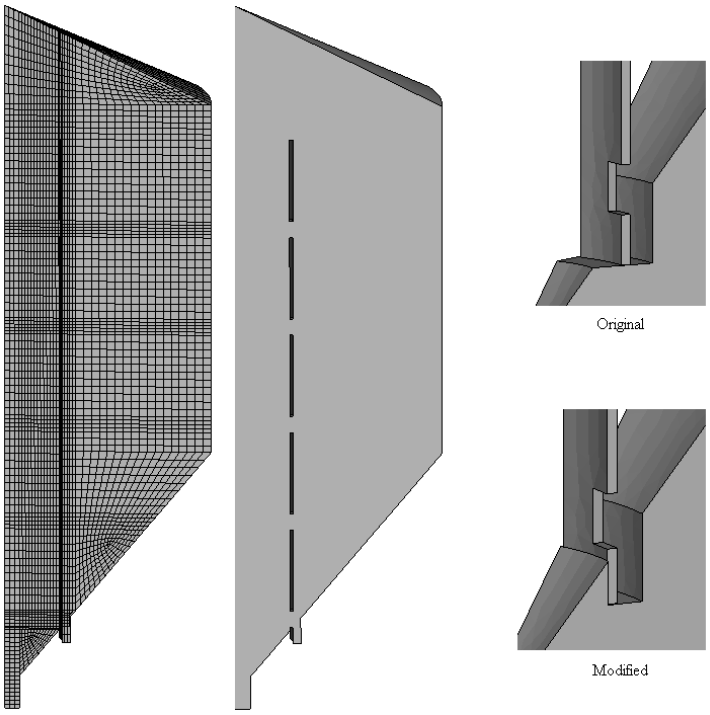

Figure 7.4: *The model of the pellets in the improved design 1 with and without the mesh and with enlargements of the modification.*

From the results, in the original design, the modification is located in an area of small velocities. As can be expected; the influence is rather small as seen in Figure 7.5. The vertical stress is decreased from 320 kPa to 300 kPa at the bottom above the plateau where the modification is present. The principal stress is increased from 370 kPa to 390 kPa at the openings. This can be the effect of a somewhat higher velocity outside the pipe flow which is causing higher shear stress.

7.3 Design modification 2 - Increased inclination in the hopper

One way to improve both the traceability and decrease the stresses is to create a pure mass flow inside the inner tube. The pellets will not be mixed when the flow profile is flat and the flowing mass will be relived directly towards the surface of the inner tube causing lower stresses.

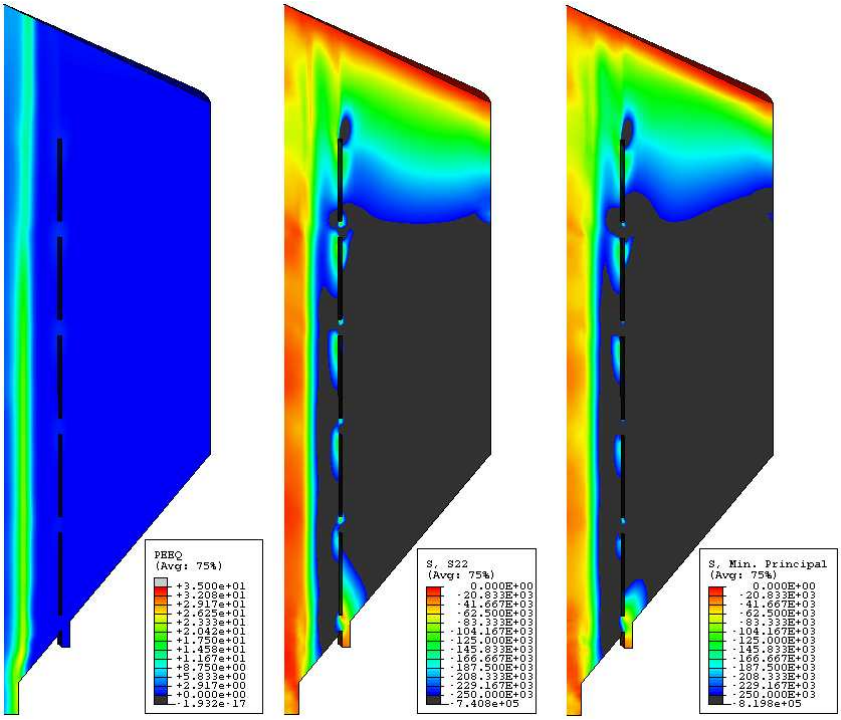

Figure 7.5: *Design modification 1. Maximum vertical stress is 300 kPa and maximum principal is 390 kPa.*

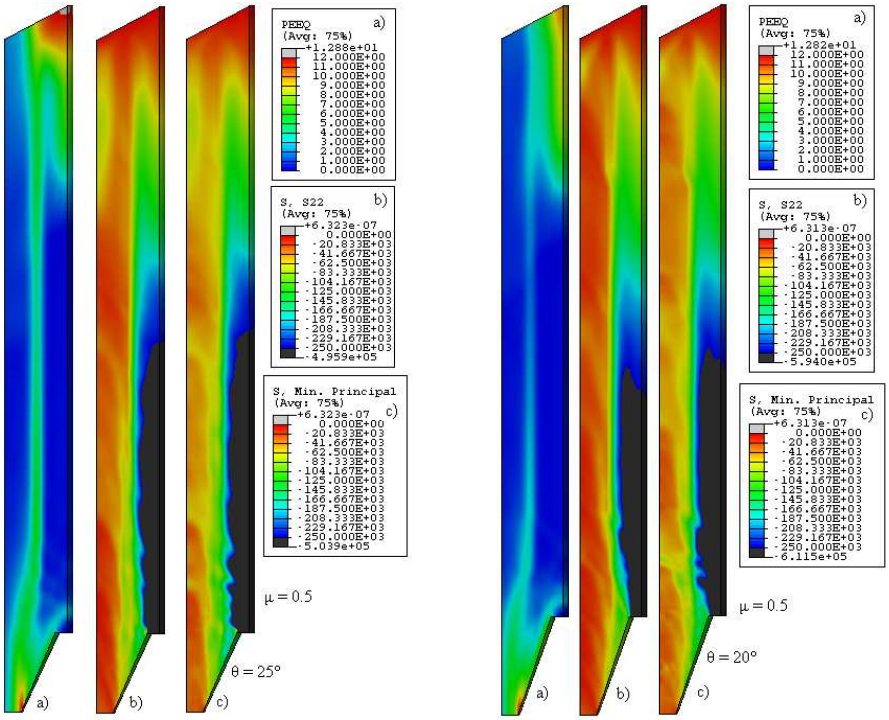

Figure 7.6: *Modification 2. The result of a hopper angle set to* 25° *and* 20° *with an overall friction coefficient set to 0.5. No pure mass flow is observed but strongly increased stress.*

To make the simulations more rational simply pellets inside the inner tube are evaluated. The simulations are performed simply to determine where it is possible to find a mass flow. The stresses are showed in the results, but are not final because the openings are not present.

The physical parameters that are affecting the flow profile are according to Figure 2.3 the internal friction, the wall friction and the slope of the walls in the hopper. It is not possible to affect the internal friction of the material. The wall friction can not be lower than the one against steel plates, which has an upper characteristic value of 0.6. Left is the inclination of the hopper. Three models assuming a hopper angle of 25°, 20° and 15° respectively are represented in Figure 7.7.

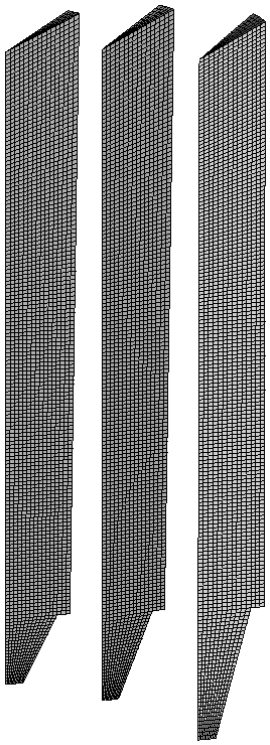

Figure 7.7: *The model of the pellets in the Design modification 2 with a hopper angle of* 25°*,* 20° *and* 15° *respectively.*

The friction coefficient is fixed at a lower bound of 0.5 and an upper bound at 0.6 in the hopper and 0.66 against the inner tube.

At a hopper angle of 25° and 20° there is no pure mass flow observed for a friction coefficient of 0.5, as seen in the Figure 7.6. As there is no mass flow at the lower bound, there is no need to investigate higher friction coefficients. When the hopper angle decreases the maximum stress is strongly increased. At a hopper angle of 15° and a friction coefficient of 0.5, there is a pure mass flow in the tube and a decrease in the stresses, but it is not sufficient. See Figure 7.8. The upper bound is also simulated and represented in the same picture showing a good result in terms of stress, but the combined pipe and mass flow is again obtained.

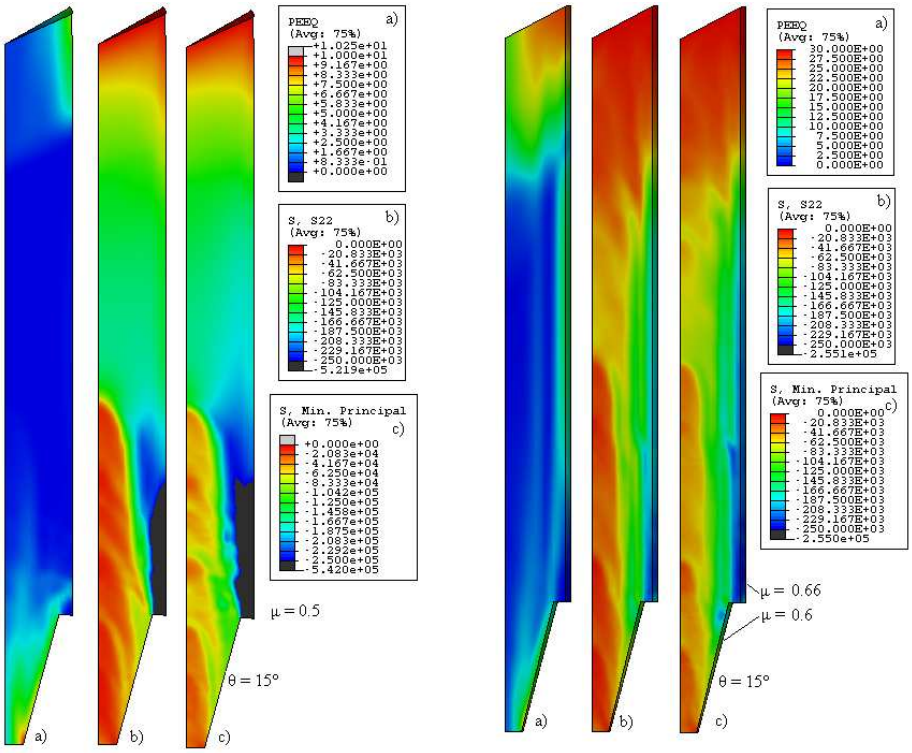

Figure 7.8: *Design modification 2. The result of a hopper angle set to 15 degrees with lower bound* $\mu = 0.5$ *gives mass flow but upper bound* $\mu = 0.6/0.66$ *does not.*

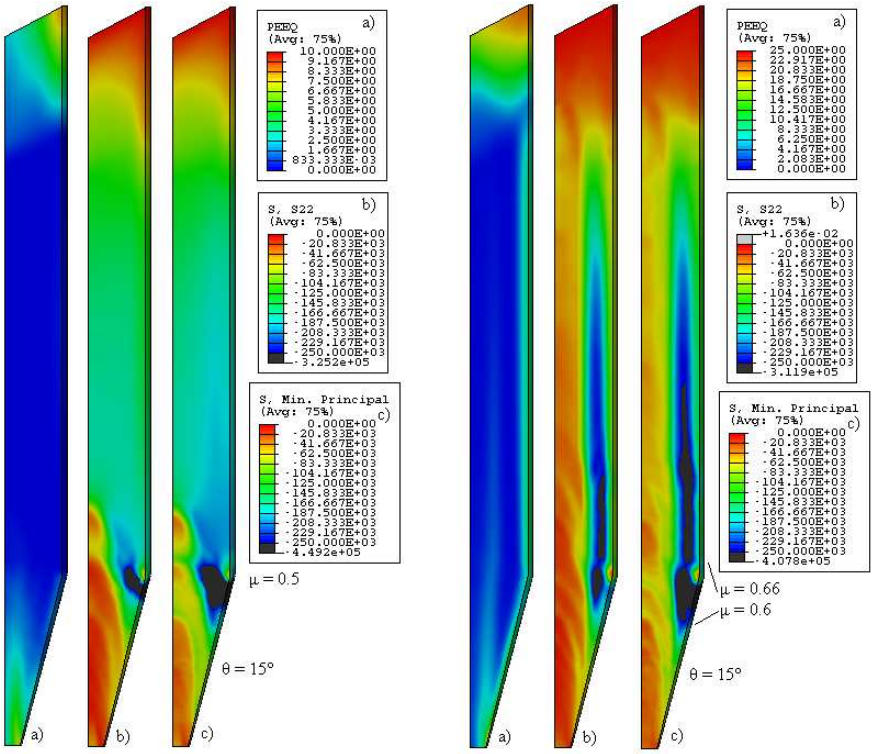

Figure 7.9: *Design modification 2. The result of a complete oblique hopper angle set to 15 degrees with lower bound* $\mu = 0.5$ *gives mass flow but* $\mu = 0.6/0.66$ *does not.*

In Figure 7.9 the pellets inside the inner tube are simulated without the presence of the plateau and at a hopper angle of 15°, both at the lower and upper bound of the friction coefficient. The figure shows that both higher stresses and the combined funnel and mass flow is obtained without the influence of the plateau at this hopper angle.

By the original drawings in appendix A it can be noticed that the smallest angle possible is 25°. If lower angles are needed the underlaying tunnel has to be lowered or the diameter of the inner tube has to be smaller.

7.4 Design modification 3 - Varying thickness of the inner tube

The inner tube has to be thicker in the bottom than 300 mm to stand the bending moment from an eccentric load. The preliminary dimension is 800 mm at the bottom.

An oblique inner side is expensive but might be effective. The more practical and economical choice is to make the indentation stepwise. This is investigated in two different ways. One with an indentation of 5 cm each 5 meter and one with an indentation of 12 cm a each 10 meter. The three modifications are shown in Figure 7.10. The overall friction coefficient is 0.5 and the the Drucker-Prager material parameter β is 46°.

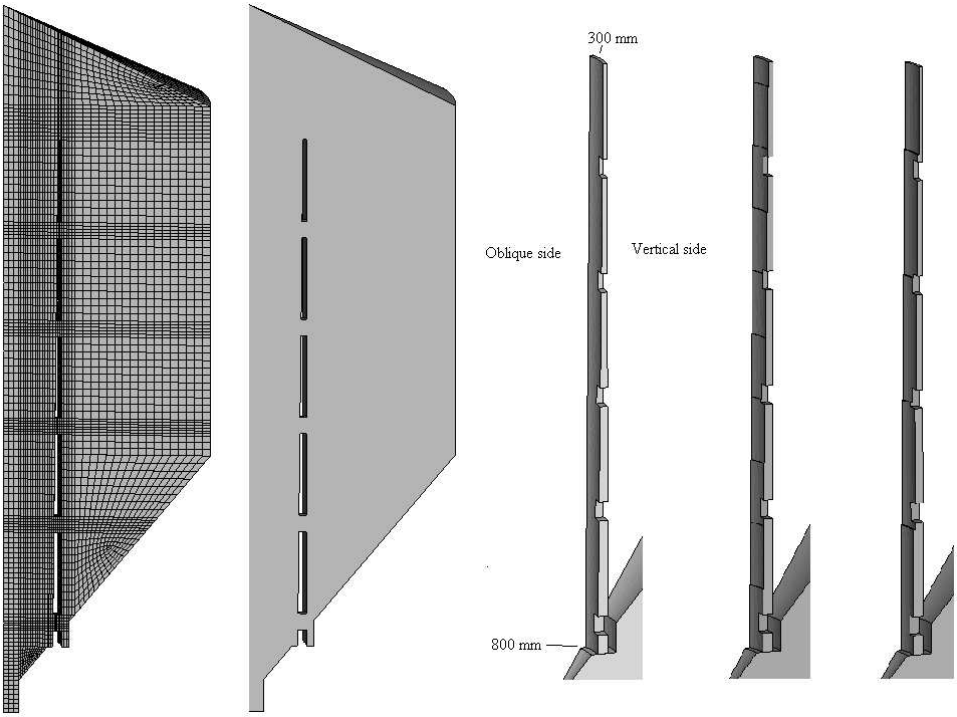

Figure 7.10: *The model and mesh of the oblique and stepped simulations.*

From the results in Figure 7.11, 7.12 and 7.13 it can be seen that the oblique side is not more effective than the stepped option with an indentation of 5 cm each 5 m. Both have a maximal vertical stress at 300 kPa above the plateau and a maximal principal stress

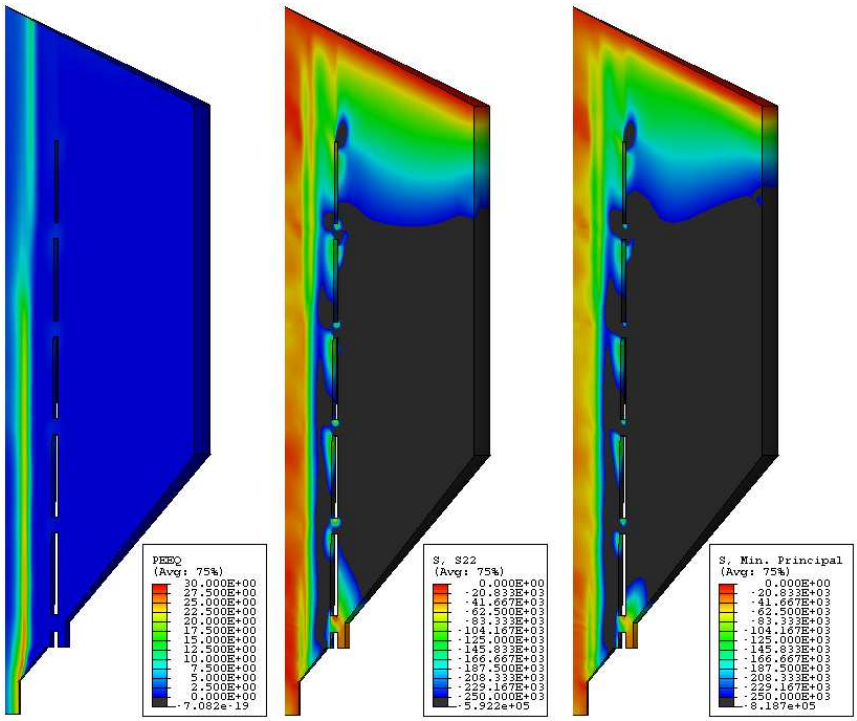

Figure 7.11: *Design modification 3. The result of the inner tube with an oblique side. Maximum vertical stress is 300 kPa and maximum principal stress 360 kPa.*

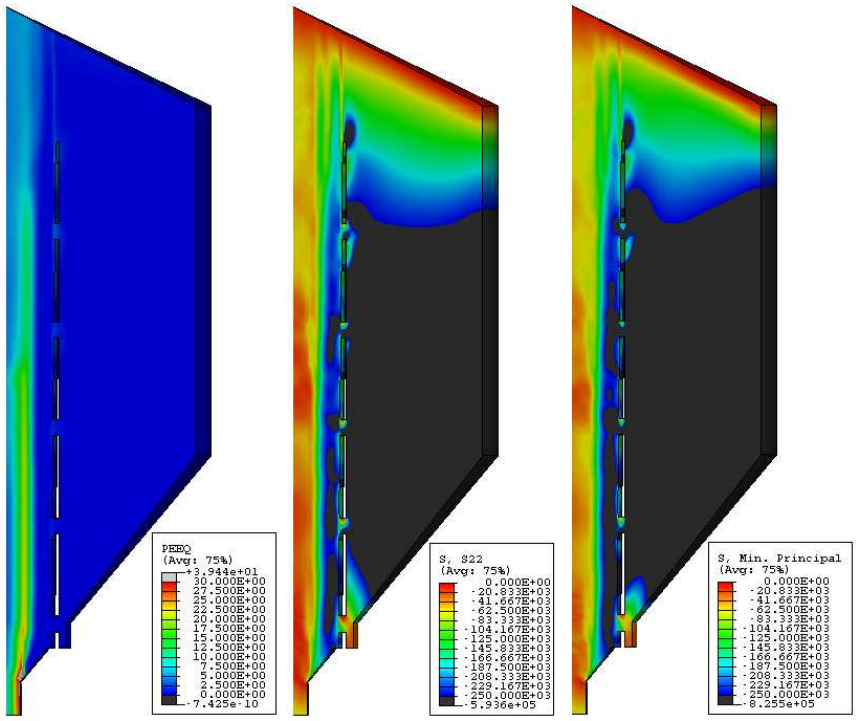

Figure 7.12: *Modification 3. The result of the inner tube with an indentation of 5 cm each 5 m. Maximum vertical stress is 300 kPa and maximum principal stress is 370 kPa.*

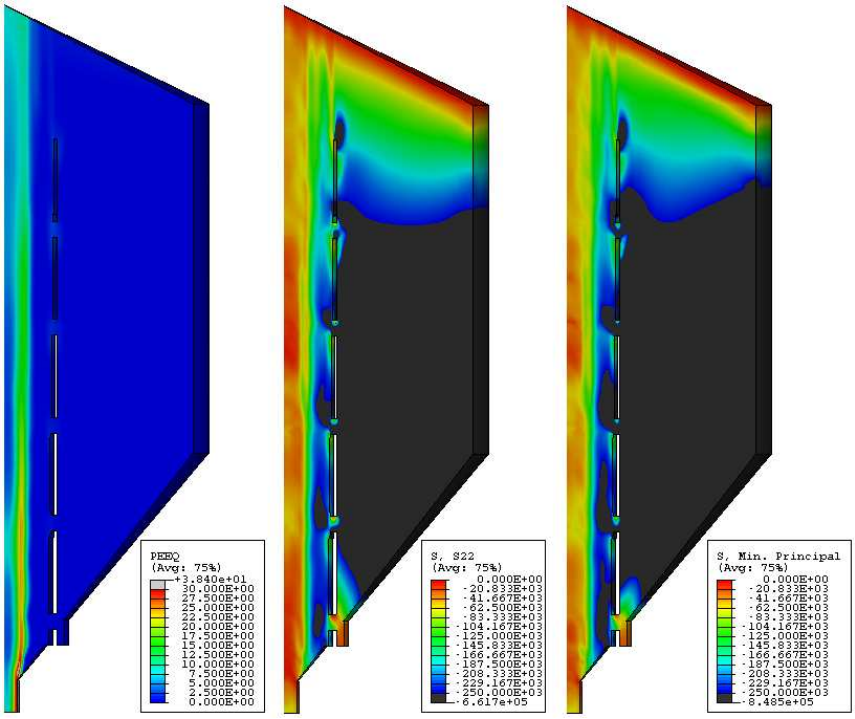

Figure 7.13: *Modification 3. The result of the inner tube with an indentation of 12 cm each 10 m. Maximum vertical stress is 330 kPa and maximum principal stress is 420 kPa.*

around 360 kPa outside the upper openings. The last alternative with an indentation of 12 cm each 10 m shows higher maximal stresses than the other two. Maximum vertical stress is 330 kPa and maximum principal stress is 420 kPa.

The flow is still a combined pipe and mass flow as can be expected with this type of modification, as it intends to increase the friction forces along the walls of the inner tube.

7.5 Design modification 4 - Shorter inner tube

The inner tube is an expensive part of the project. A question that appear is what happens if the tube is shorter than the original one. The simulations are performed with a shortening of the inner tube in steps of 9.1 meter, which is the repeated length in the design as seen on the drawings in Appendix A. The model and the mesh are almost the same as for the previous preformed simulations but with a shorter inner tube. The overall friction coefficient is 0.5 and the the Drucker-Prager material parameter β is 46°.

From the simulations on the original design it can be seen that the stress limit outside the tube is in level with the upper opening. In the result shown in Figure 7.14 it is found that the modification has small influence. The vertical stress is decreased with 20 kPa to 300 kPa from the original design. The pellet to pellet interaction, over the inner tube, is probably stronger than the interaction between pellet and the inner tube. The maximum principal stress is still 370 kPa.

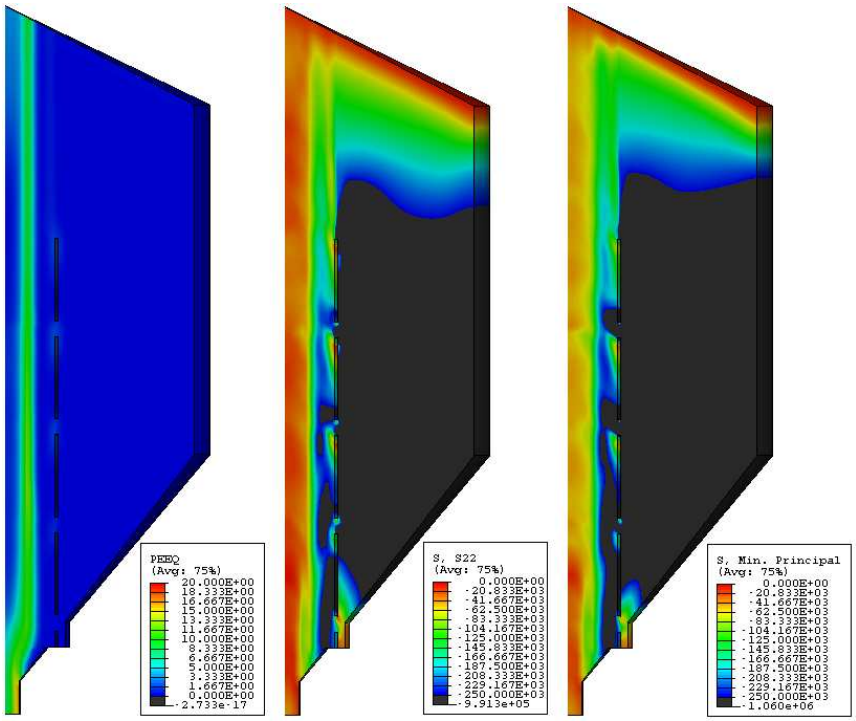

Figure 7.14: *Design modification 4. The result of a 9.1 m shorter inner tube. Maximum vertical stress is 300 kPa and maximum principal stress is 370 kPa.*

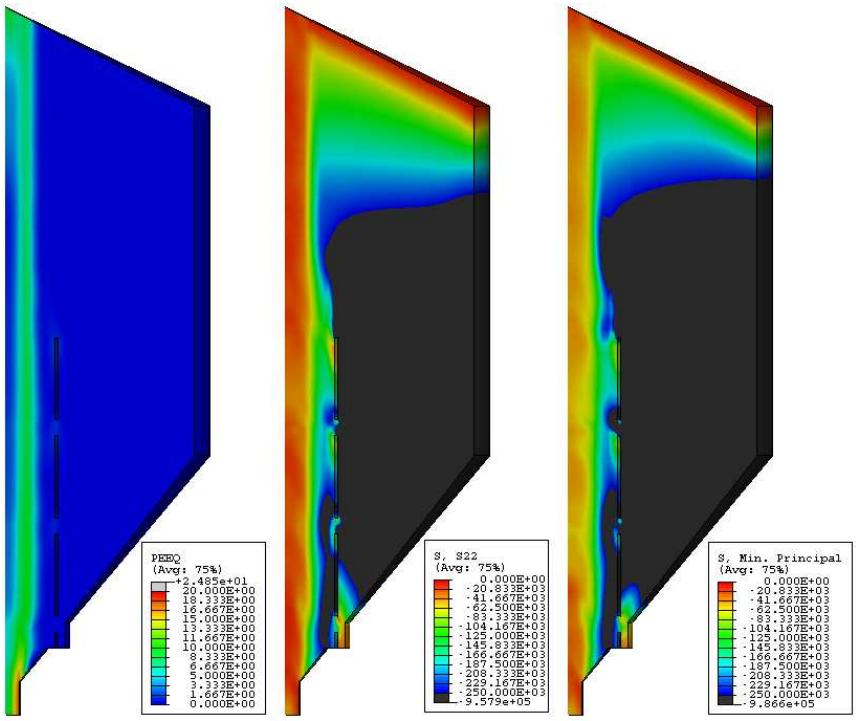

Figure 7.15: *Design modification 4. The result of a 18.2 m shorter inner tube. Maximum vertical and principal stress is 350 kPa at the top of the inner tube.*

When shorting the tube, by 18.2 m, the principal stress downwards the tube is also lowered with 50 kPa to 320 kPa. But now there is an area at the top of the silo which has maximum vertical and principal stress at 350 kPa.

7.6 Design modification 5 - Decreased radius of the inner tube

As seen from Design modification 2 with increased inclination in the hopper an inclination lower than 15° is needed to obtain mass flow for the upper bound of the friction coefficient. The lower bound would on the other hand give very high stresses.

This section investigates the influence a smaller radius of the inner tube has on both the flow pattern and the stresses. What happens is that both the ratio between the areas in the bin and the outlet and the ratio between the frictional surface of the tube and the volume of the pellets change. The original radius of the inner tube is 5 meter. The radius of the outlet is fixed at 1.35 meter.

From simulations with different radius and hopper angles combined with the friction coefficient are four results chosen to represent the result. At a lower bound of 0.5 and a upper bound of 0.6 in the hopper and 0.66 in the tube . The models are shown in Figure 7.16.

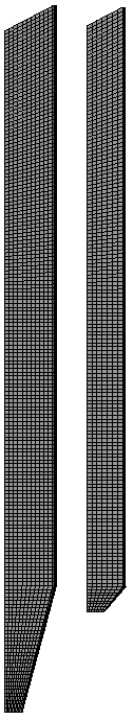

Figure 7.16: *The models of pellet inside the inner tube. Left: A radius of 4 meter and a hopper angle of* 15°. *Right: A radius of 3 meter and a hopper angle of* 40°.

The simulations with a radius set to 4 meters shows, for most combinations of hopper angles, a combined flow but with a more even velocity profile than earlier. The outflow is

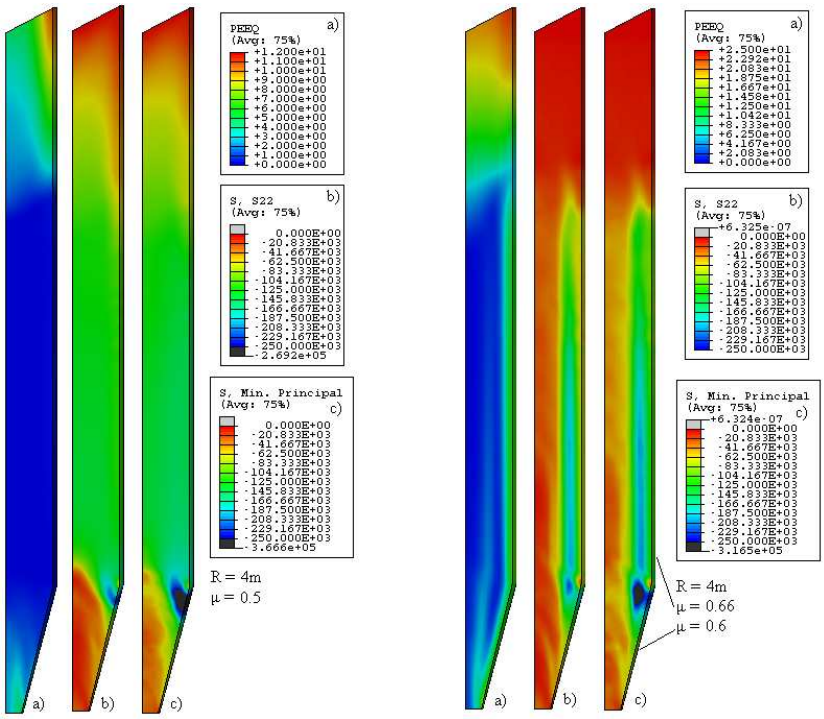

Figure 7.17: *Modification 5. Radius = 4 meter and hopper angle = 15°. Mass flow is obtained at the lower bound and with a moderate combined flow at the upper bound.*

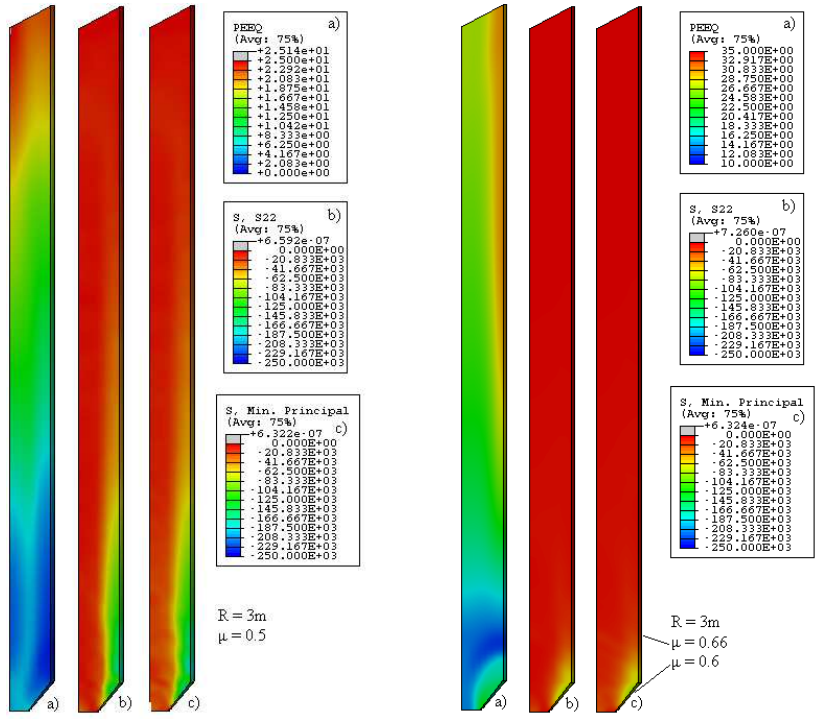

Figure 7.18: *Modification 5. Radius = 3 meter and original hopper angle = 40°. Mass flow is obtained at both the lower and upper bound of the frictional coefficient.*

still mixed with about 10% pellets but as the velocities are more equal improves this the traceability. Only at a hopper angle of 15° is a pure mass flow is obtained for the lower bound, at the upper bound is there a moderate combined flow. The simulations with a radius set to 4 meters and a hopper angle of 15° is presented in Figure 7.17.

The stresses are at a hopper angle of 40° about 360 kPa in both directions and at a hopper angle of 25° as high as 400 kPa vertical and 450 kPa in principal direction.

In Figure 7.18 the result is shown from a simulation with an inner radius of 3 meter and a hopper angle of 40° which is the original angle. For this radius mass flow is obtained, even moderate at the upper bound of the frictional coefficient. According to the simulation with the lower bound maximum vertical stress is 205 kPa and the maximum principal stress is 215 kPa. At the upper bound of the frictional coefficient both the maximmum vertical and maximum principal stress is as low as about 85 kPa.

The ratio between the radius in the bin and at the outlet has, according to these simulations, influence on the flow pattern.

Part IV

Summary

Chapter 8

Summary

The vertical and principal stresses and the flow pattern from simulations on the original design and with modifications are compiled below. Not all of the modification designs are presented but those who are considered most interesting.

Model	*Vertical*	*Principal*	*Flow*	*Note*
Original Design state 1	320	370	Comb.	A full silo with an inner tube.
Original Design state 2	305	335	Comb.	The pellets surface is at the top of the inner tube.
Original Design state 3	315	350	Comb.	The pellets surface is outside the tube at the top of the tube and at the first opening inside.
Modification 1	300	390	Comb.	A full silo with an oblique plateau
Modification 2	-	-	Comb.	Increased inclination in the hopper, various results at very high stresses.
Modification 3	300	360	Comb.	Varying thickness of the inner tube. Result from an indentation of 5 cm each 5 meter.
Modification 4	300	370	Comb.	A shorter tube. Results from a 9.1 meter shorter tube.
Modification 5	205	215	Mass	Decreased radius of the inner tube. Result from a radius at 3 meter where mass flow is obtained.

8.1 Conclusions

The original design has a combined pipe and mass flow inside the inner tube but no movements in pellets outside the tube. The pellets in the outlet are mixed with about 10% pellets with uncertain origin. The stresses are higher than the limit at 250 kPa in both vertical and principal direction. The conditions are almost the same for all three simulated states making it an issue during a noticeable time. None of the smaller modifications on the original design shows any big improvement but are of interest as basics for decisions.

The only modification that shows improvement is the one with an inner tube with a smaller radius than the original 5 meter. At a radius of 3 meters, mass flow is obtained even for the original hopper angle at 40° together with low stresses.

The wall friction coefficient and the angle of internal friction in the pellets have influence on the result. Higher friction coefficients give lower stress but counteract mass flow. Low friction coefficients tend to give mass flow but with high stresses. The internal friction angle in the pellets, influence in such a way that it gives mass flow at low values and higher stress at higher values.

8.2 Discussion

The silo with the original design will probably have no problem with the stress levels as the threshold is chosen with good margin, but from an economical point of view this margin is of interest. With a more detailed knowledge about the causes of the quality decreasing in the pellets during mechanical influence, maybe a more custom made design is possible or a design that can have an increased focus on the pellets' quality. Better knowledge in the effects of stress influence on iron ore pellets will lead to a better economical use. There is a possibility that this knowledge will have large benefits as it is the most uncertain parameter in the simulations.

The parameters in the simulations that affect the result on a specific geometric design are the wall frictional coefficient and the internal friction angle. The more exact the parameters are known, the more accurate the simulations will be. In this thesis they have been executed with friction coefficients from the European standard and not from specific tests.

The most attractive design of the tube identified from the simulations is the one with a smaller radius than the original. The smaller radius gives mass flow for high friction coefficients and lower stresses. A smaller radius, however, gives the tube a decreased moment of inertia and will therefore probably meet engineering problems.

A lower tube is shown possible and should decrease the bending moment in the tube which is a cantilever beam. To avoid problems caused by decreased moment of inertia, the tube can be supported by beams or stays made of wires in the top. At the bottom it can be supported with plates from the bedrock. With a smaller radius it may also be possible to construct the inner tube out of steel instead of concrete.

8.3 Future work

It is of interest to verify the simulation method in the current work. Not only the stresses and the flow pattern should be verified but also the material model. It is of importance to verify the simulations with both practical experiments and observations in full scale. The most interesting observation is if the pellets outside the pipe flow really have a flow towards the pipe flow through the transition zone. This flow is what causes the mass flow outside the pipe flow in areas with high stresses. If there is no such flow the inner tube will be unnecessary.

Experiments on iron ore pellets' material parameters should be performed, to make them more accurate. This will lead to better simulation conditions and to a more realistic result.

From the discussion, it is possible to obtain a more detailed knowledge of the causes to the quality decrease in the pellets during mechanical influence. The increased knowledge can lead to a more economical, or from a stress point of view, better design.

References

Bibliography

[1] European Committee for Standardization, *Eurocode 1, Part 4: Actions on Silos and Tanks,* Central Secetariat, Brussels 2002

[2] ABAQUS Inc. *ABAQUS Analysis Manual V6.6,* www.gorkon.byggmek.lth.se/v6.6, 2007

[3] ABAQUS Inc. *Getting Started with ABAQUS/Explicit: Keywords Version V6.6,* www.gorkon.byggmek.lth.se/v6.6, 2007

[4] Gustafsson, Gustaf, *Simulation and Modelling of Pellets in Large Storing Systems,* Master's Thesis LTU 2006:218 CIV, Luleå 2006

[5] Karlsson, Tomas, *Finite Element Simulation of Flow in Granular Materials,* Research report, TULEA 1995:32, Luleå 1995

[6] Knutsson, Sven, *Measurments on Iron Ore Pellets,* Power Point Presentation at a meeting in Narvik 2006-01-29, Luleå 2006

[7] Saabye Ottosen, Niels and Ristinmaa Matti, *The Mechanics of Constitutive Modeling,* Elsevier 2007

[8] Martens, Peter, *Silo Handbuch,* Ernst und Sohn, Berlin 1988

A - Original drawings

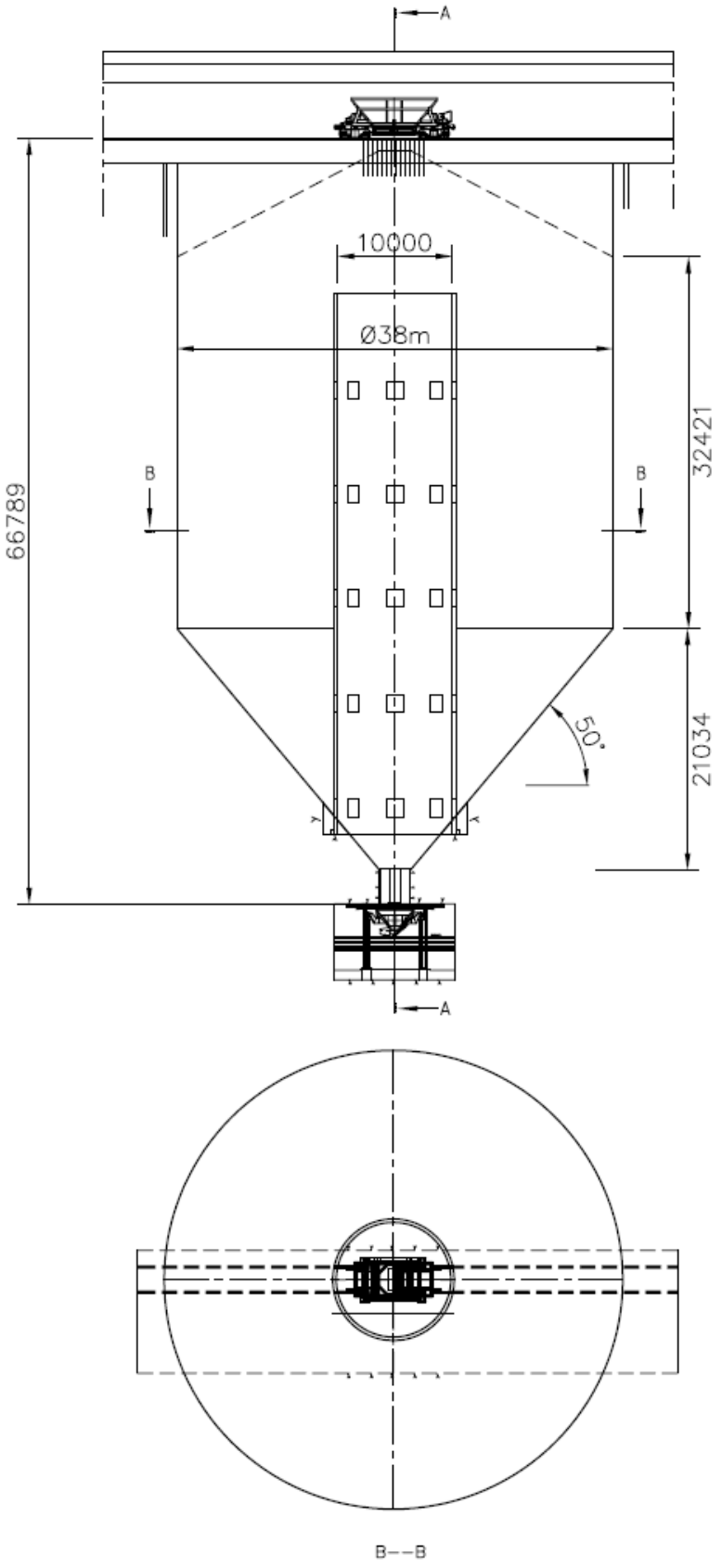

Figure 8.1: *Original drawing of the silo.*

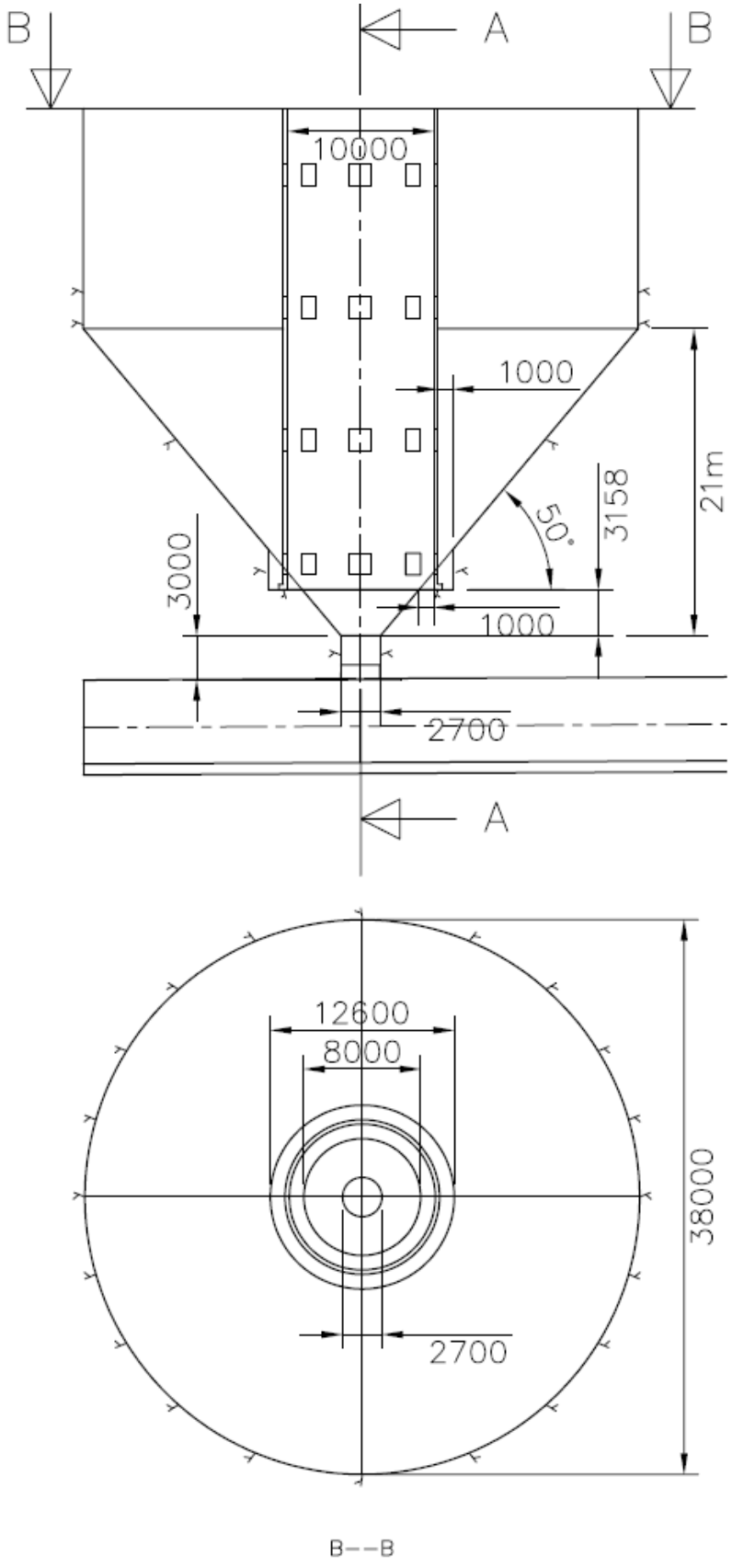

Figure 8.2: *Original drawing of the silo.*

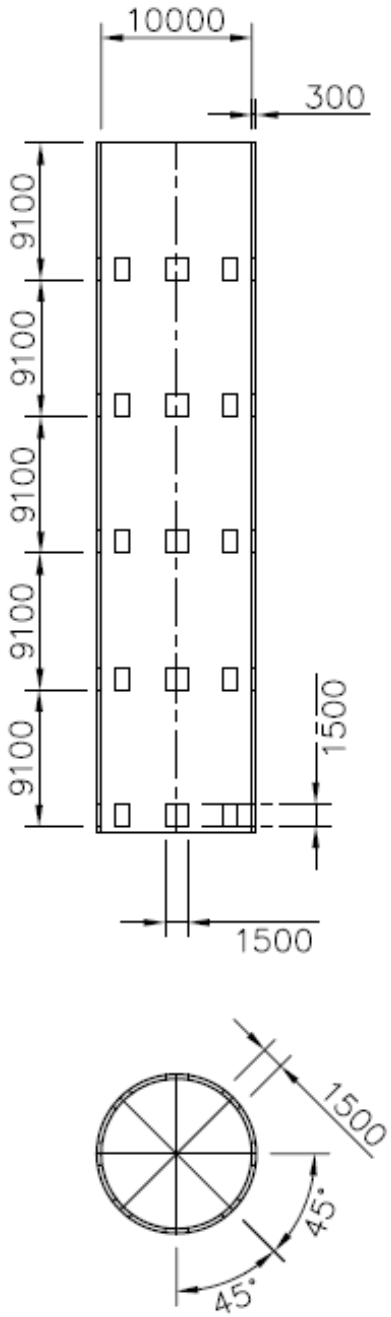

Figure 8.3: *Original drawing of the inner tube.*